Annu. Rev. Fluid Mech. 2003. 35:183–227
doi: 10.1146/annurev.fluid.35.101101.161125
Copyright © 2003 by Annual Reviews. All rights reserved

PARTICLE-TURBULENCE INTERACTIONS IN ATMOSPHERIC CLOUDS

Raymond A. Shaw
Department of Physics, Michigan Technological University, Houghton, Michigan 49931; email: rashaw@mtu.edu

Annu. Rev. Fluid Mech. 2003.35:183-227. Downloaded from www.annualreviews.org
by Fordham University on 01/19/13. For personal use only.

Key Words cloud physics, turbulence, multiphase flows

■ **Abstract** Turbulence is ubiquitous in atmospheric clouds, which have enormous turbulence Reynolds numbers owing to the large range of spatial scales present. Indeed, the ratio of energy-containing and dissipative length scales is on the order of 10^5 for a typical convective cloud, with a corresponding large-eddy Reynolds number on the order of 10^6 to 10^7. A characteristic trait of high-Reynolds-number turbulence is strong intermittency in energy dissipation, Lagrangian acceleration, and scalar gradients at small scales. Microscale properties of clouds are determined to a great extent by thermodynamic and fluid-mechanical interactions between droplets and the surrounding air, all of which take place at small spatial scales. Furthermore, these microscale properties of clouds affect the efficiency with which clouds produce rain as well as the nature of their interaction with atmospheric radiation and chemical species. It is expected, therefore, that fine-scale turbulence is of direct importance to the evolution of, for example, the droplet size distribution in a cloud. In general, there are two levels of interaction that are considered in this review: (*a*) the growth of cloud droplets by condensation and (*b*) the growth of large drops through the collision and coalescence of cloud droplets. Recent research suggests that the influence of fine-scale turbulence on the condensation process may be limited, although several possible mechanisms have not been studied in detail in the laboratory or the field. There is a growing consensus, however, that the collision rate and collision efficiency of cloud droplets can be increased by turbulence-particle interactions. Adding strength to this notion is the growing experimental evidence for droplet clustering at centimeter scales and below, most likely due to strong fluid accelerations in turbulent clouds. Both types of interaction, condensation and collision-coalescence, remain open areas of research with many possible implications for the physics of atmospheric clouds.

1. INTRODUCTION

1.1. Broader Implications of Cloud Physics

When viewed from space, the Earth reveals much more cloud and ocean than earth. Indeed, the presence of clouds is a crucial aspect of hydrological and radiative balances necessary for the existence of life on Earth. Furthermore, a perusal of

art in the world's great museums and galleries reveals that the qualitative features of clouds have not undergone any radical change over the last few hundred years. Yet there is evidence that the formation, extent, and duration of clouds can be altered by anthropogenic or biological influences. In response to these facts, "the factors controlling the distribution of clouds and their radiative characteristics" is included in the Intergovernmental Panel on Climate Change (IPCC 1996) list of "most urgent scientific problems requiring attention."

One of the intriguing (and difficult) aspects of the cloud-climate problem is the fundamental importance of processes occurring on extremely small scales in determining the macroscopic properties of clouds, including their lifetime, extent, precipitation efficiency, and radiative properties. Thus, if we are to understand the role of clouds in human affairs and the global environment, we are obliged to increase our understanding of processes occurring on seemingly unrelated scales, such as cloud-droplet activation and the subsequent temporal and spatial evolution of cloud-particle size distributions. The formation of cloud droplets on individual aerosol particles of varying chemical composition, the subsequent growth by vapor condensation, and then the collision and coalescence of cloud droplets, all processes occurring on micrometer to millimeter scales, eventually take part in determining the macroscopic properties of a cloud such as its precipitation efficiency and its optical properties.

Even casual observations of convective clouds, such as that shown in Figure 1, reveal that such clouds are turbulent, are inherently three dimensional, tend to

Figure 1 A turbulent cloud, illustrating the great range of spatial scales and the sharp boundaries characteristic of such a system. Similarly, a series of pictures taken in succession would illustrate the large range of temporal scales.

Annu. Rev. Fluid Mech. 2003.35:183-227. Downloaded from www.annualreviews.org
by Fordham University on 01/19/13. For personal use only.

Annu. Rev. Fluid Mech. 2003.35:183-227. Downloaded from www.annualreviews.org
by Fordham University on 01/19/13. For personal use only.

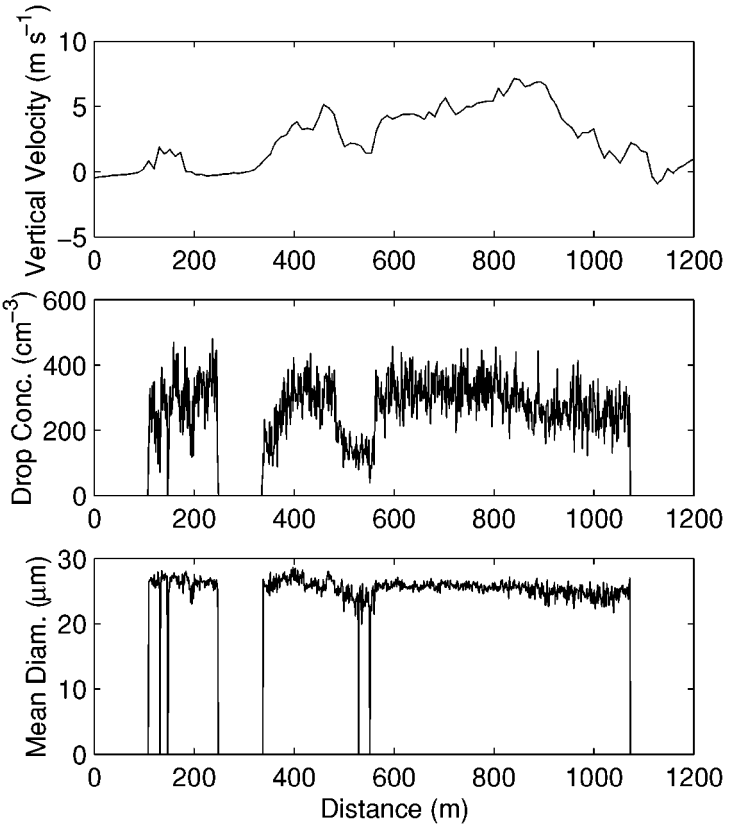

Figure 2 A traverse through a cumulus cloud. The top panel shows the vertical velocity, the middle panel shows droplet number density, and the bottom panel shows mean droplet radius. Note the sharp edges characteristic of the cloud-environment mixing process. Note also that to a large extent the mean radius fluctuates between a constant value and zero, implying that dry and cloudy air are largely segregated during much of the mixing process. Data from the SCMS field experiment, courtesy of J.-L. Brenguier, Meteo-France.

have sharp transitions from cloudy to clear air, evolve over a huge range of spatial and temporal scales, and consist of highly dispersed condensed-phase water. Quantitative measurements, such as those shown in Figure 2, confirm this general picture. These features lead to at least four characteristics of clouds that determine how they interact with other components of the Earth system. (*a*) Clouds represent the highest mass concentration of any atmospheric aerosol (Twomey 1977). In addition, they possess an enormous surface area and therefore are of great importance for heterogeneous chemistry and aerosol processing and removal. (*b*) Clouds are extremely effective in their interaction with visible and infrared radiation. In the visible range, light is redistributed mainly by scattering, and in the infrared,

clouds are close to being black bodies and therefore modify the transfer of infrared (terrestrial) radiation through the atmosphere (Twomey 1977). (*c*) Clouds can become "colloidally unstable" and form raindrops large enough to fall to the ground and therefore form a fundamental link in the hydrologic cycle. (*d*) Clouds play a crucial role in transporting water and energy in the atmosphere, especially vertical transport.

Each of these items is inherently linked to the formation and evolution of cloud-droplet size distributions. As a result, understanding how the size distribution varies spatially and temporally in a cloud is one of the major challenges in the atmospheric sciences. The role of fine-scale turbulence in the evolution of cloud-droplet size distributions is the focus of this review.

Annu. Rev. Fluid Mech. 2003.35:183-227. Downloaded from www.annualreviews.org
by Fordham University on 01/19/13. For personal use only.

1.2. Scope: Turbulence-Cloud Interactions on Small Scales

It was realized during the infancy of cloud physics as a discipline that turbulence likely would play a role in the evolution of a cloud, both at macro- and microscales (see Vohl et al. 1999, Section 1, for a brief summary of some of the earliest references). Today, the role of turbulence in cloud formation and dissipation is a major research problem, with in situ, computational, laboratory, and theoretical tools being applied to all scales of the problem. Although it is somewhat artificial to separate "large" and "small" scales in a cloud, we do so here simply to limit the scope of this review. Questions of large-scale entrainment and turbulent fluxes of energy and water vapor, although of great interest, are not addressed here. Instead, we focus on the interaction of turbulence with particles at the smallest scales in a cloud. This is an active area of research that lies at the interface between turbulent fluid mechanics and cloud physics, and the purpose of this review is not to give a thorough overview of either turbulence or the microscale physics of clouds, nor is it to create a false impression that the major problems have been solved. Rather, the intention is to provide an introduction to the basic problems lying at this interface of two fields and the current and recent research aimed at answering those questions, as well as some thoughts on possible future directions. Finally, again for the sake of limiting the scope of this review, we focus on "warm clouds," meaning clouds that contain only liquid water (noting, of course, that the fundamental physics applies to more complex situations where ice particles are present).

A physically based justification for limiting our view to interactions that take place primarily at the smallest spatial scales in a cloud exists. These scales are fundamental to the microscale physics of droplet growth, which determines spatial and temporal variations in the droplet size distribution. In turn, the droplet size distribution is the defining characteristic of a cloud, determining how the cloud interacts with electromagnetic radiation, how fast precipitation will form, and so forth. For example, droplet collisions and the relevant fluid motions influencing their efficiency occur on scales on the order of 10^{-3} m or smaller. Similarly, the local thermodynamic environment of a cloud droplet, which determines the rate at which the droplet grows owing to condensation, is characterized by spatial scales on the

order of 10^{-3} or smaller. Fundamentally, these scales are determined by molecular diffusivities for mass, energy, and momentum transport, all of which have similar magnitudes in a cloud. The same quantities determine the dissipation scale of a turbulent flow, also on the order of 10^{-3} m for a cloud, so it is no coincidence that these scales have similar magnitudes and that the processes interact. Always keeping in mind that the smallest scales are linked inherently to the macroscopic properties of the cloud, we focus on the small scales to understand the physics of those interactions.

We note that several other recent reviews covering various aspects of cloud-turbulence interactions are well worth consulting for their differing perspectives. The problem of rain formation in warm clouds is carefully reviewed by Beard & Ochs (1993), with many topics considered, including the role of turbulence. The physics of entrainment of dry air into clouds and its relevance to cloud evolution is reviewed by Blyth (1993). A broad review of turbulence effects on the growth of cloud droplets aimed primarily at the cloud physics community is that by Jonas (1996). Recent advances made in understanding the role of particle inertia in the microscale physics of clouds are reviewed by Pinsky & Khain (1997b). A review by Vaillancourt & Yau (2000) covers aspects of cloud particle interactions with turbulence, especially "preferential concentration" and the overlap with ongoing research in the broader area of multiphase flows. Finally, Lamb (2001) gives a concise introduction to the amazing breadth of the "rain production" problem.

Because this review is meant for a broad audience with readers beyond the boundaries of cloud physics, in Section 2 we give a brief overview of the essential physics of cloud formation and the processes governing the spatial and temporal evolution of the cloud-droplet size distribution. In Section 3 we address the nature of turbulence in clouds, and we discuss how clouds are described as random systems containing a countable scalar constituent (cloud droplets). The equation of motion for a cloud droplet and discussions of mechanisms by which number density fluctuations can arise are presented in Section 4. Recent research on the role of fine-scale turbulence in the condensation growth process is described in Section 5, and on the collision growth process in Section 6. Measurements of cloud properties at sub-m scales are discussed in Section 7, and some final remarks on outstanding problems are given in Section 8.

Annu. Rev. Fluid Mech. 2003.35:183-227. Downloaded from www.annualreviews.org
by Fordham University on 01/19/13. For personal use only.

2. THE CLOUD-DROPLET SIZE DISTRIBUTION

Cloud droplets initially form on preexisting aerosol particles that serve as condensation nuclei. As long as a supersaturated environment is maintained—for example, as a result of the continual cooling of air doing work against Earth's gravitational field as it rises—the cloud droplets formed on individual aerosol particles will continue to grow by water vapor condensation. At this point, the cloud is sometimes said to be colloidally stable because of the relatively small growth rates typically attained owing to condensation alone. To achieve the explosive growth

Annu. Rev. Fluid Mech. 2003.35:183-227. Downloaded from www.annualreviews.org
by Fordham University on 01/19/13. For personal use only.

necessary to produce particles large enough to fall from a cloud during the extent of its lifetime, cloud droplets must begin to collide and coalesce. Identifying how this process begins and the rate at which it occurs is one of the major challenges of cloud physics. Precipitation formation is just one example of a process that is sensitive to spatial and temporal variations of the cloud-droplet size distribution. The essential processes governing the size distribution evolution are discussed in this section to provide background for reviewing the role of fine-scale turbulence in these processes.

If a single droplet is chosen at random from a volume containing many cloud droplets, $p(r)$ is the probability of choosing a droplet with radius between r and $r + dr$ (e.g., Jameson & Kostinski 2001, Seinfeld & Pandis 1998); $p(r)$ is a probability density, properly normalized such that $\int_0^\infty p(r)dr = 1$. The cloud-droplet size distribution is defined as $f(r) = np(r)$, where n is the number density of droplets (of all radii) in the volume. Because cloud volumes and (of greater relevance) the sampling volumes of instruments are finite, the size distribution $f(r)$ can only be estimated, and the ability to do this depends on the statistical homogeneity (or stationarity) of the cloud (e.g., Jameson & Kostinski 2001, Liu & Hallett 1998).

Perhaps the main challenge of cloud physics is to determine $f(r)$ as a function of position and time. This is made more complex when the thermodynamic phase (liquid water versus ice) is taken into consideration, but here we focus on the liquid phase only. The dynamic equation for the droplet size distribution, given several assumptions that are discussed later, can be written as

$$\frac{\partial f(r)}{\partial t} = J - \frac{\partial[\dot{r} f(r)]}{\partial r} - \int_0^\infty \kappa(r, r')\, f(r)\, f(r')\, dr' + \frac{1}{2}\int_0^r \left(1 - \frac{r'^3}{r^3}\right)^{-2/3} \kappa((r^3 - r'^3)^{1/3}, r')\, f((r^3 - r'^3)^{1/3})\, f(r')\, dr'. \quad (1)$$

This is, essentially, a form of the Boltzmann transport equation (e.g., Reif 1965). We consider the physical meaning of each term separately. The first term on the right side is a particle source term, written as a nucleation (or activation) rate J. The second term can be expanded into $-\dot{r}\frac{\partial f(r)}{\partial r}$, which is the shift in $f(r)$ due to droplet growth by condensation, and $-f(r)\frac{\partial \dot{r}}{\partial r}$, which represents the tendency for a size distribution to become narrower as condensation growth occurs (see Equation 2). The condensation growth rate for a single droplet is obtained by considering a diffusive flux of water vapor from the surrounding air to the spherical surface of the droplet and the resulting energy flux from the droplet surface to the surrounding air due to the large enthalpy of vaporization of water. These fluxes are coupled by conservation of energy and the Clausius-Clapeyron equation relating the droplet temperature to its equilibrium vapor pressure (e.g., Rogers & Yau 1989). For sufficiently large droplets and the small supersaturations that typically exist in the atmosphere, the droplet growth rate is

$$\frac{dr}{dt} = \gamma \frac{s}{r}, \quad (2)$$

Annu. Rev. Fluid Mech. 2003.35:183-227. Downloaded from www.annualreviews.org
by Fordham University on 01/19/13. For personal use only.

where γ is a function of environmental conditions such as temperature. Supersaturation is defined as $s \equiv p_v/p_v^* - 1$, where p_v is the vapor pressure of water and p_v^* is the *equilibrium* vapor pressure of water. Especially relevant to the discussion here is that the droplet growth rate is inversely proportional to the droplet radius. It is this dependence that forces the term $-f(r)\frac{\partial \dot{r}}{\partial r}$ to be positive, leading to a continual narrowing of the droplet size distribution $f(r)$ during condensation growth.

Supersaturation is directly related to the Gibbs free energy difference between the vapor and condensed phases and therefore is the fundamental driver of droplet growth. The time dependence of supersaturation in a volume of cloud is given by

$$\frac{ds}{dt} = \varphi u_z - \frac{s}{\tau_s}. \tag{3}$$

The derivation of Equation 3 is based on equations for conservation of energy and conservation of mass (water), as well as the droplet growth equation, the hydrostatic equation, and the Clausius-Clapeyron equation (e.g., Rogers & Yau 1989). The first term on the right side is the source of supersaturation due to vertical motion in a gravitational field, with φ being a function of the vertical profile of temperature and the saturated adiabatic lapse rate. The second term on the right side is the loss due to droplet growth, with

$$\tau_s \propto \left(\int_0^\infty f(r) r \, dr \right)^{-1}. \tag{4}$$

τ_s is the phase relaxation time and represents the timescale for relaxation to $s = 0$ in the absence of the source term φu_z. If u_z is constant, Equation 3 can be solved for a quasi-steady-state supersaturation $s = \varphi u_z \tau_s$, which is reached when the total number density of droplets is constant (no cloud-droplet activation) and the mean radius changes slowly in time (owing to condensation growth).

The portion of Equation 1 that deals with collision and coalescence of droplets (third and fourth terms on the right side) is referred to variously as the kinetic equation, the coagulation equation, or the stochastic collection equation. The latter is somewhat of a misnomer because the equation always results in the same droplet size distribution at a given time when started with identical initial conditions. It does, however, account for the discreteness of the collision-coalescence process and therefore is a significant improvement over models based on the assumption of a continuous droplet phase (continuous collection equation; e.g., Rogers & Yau 1989). It has been pointed out that the kinetic equation does not account for correlations among droplets, such as exists in a poorly mixed cloud (e.g., Bayewitz et al. 1974). As noted by Bayewitz and coworkers (1974), this is especially crucial for clouds, where the rate process is sensitive to very small numbers of large droplets that may not be uniformly distributed in the cloud. An approach for including such droplet correlations is discussed in Section 6, but this is an outstanding problem that remains to be solved in a completely satisfactory way.

The implicit assumption of zero correlations in the collision-coalescence portion of Equation 1 can be revealed as follows: The expected time for any given

droplet r to experience a collision with another droplet r' is $\tau = (n_{r'}\kappa(r, r'))^{-1}$, where $n_{r'}$ is the number density of droplets of size r' and $\kappa(r, r')$ is the collision kernel, the exact functional form depending on the physical mechanism causing the collisions. (Typically, the combination of collision and coalescence is referred to as "collection," making κ the collection kernel, but for simplicity we use only the term collision.) τ is exactly analogous to the collision time in kinetic theory (e.g., Reif 1965), and when it is assumed that droplets are distributed with uniform probability, the probability density of collision times is

$$p(t) = \frac{1}{\tau} \exp\left(-\frac{t}{\tau}\right). \tag{5}$$

Annu. Rev. Fluid Mech. 2003.35:183-227. Downloaded from www.annualreviews.org
by Fordham University on 01/19/13. For personal use only.

In other words, when no correlations in droplet position exist the probability of collision is independent of the past history of the droplet and therefore is exponentially distributed (Reif 1965, Section 12.1). After each collision, $\tau(r)$ must be recalculated because the droplet radius has changed. The collision kernel has the form $\kappa(r, r') = \pi(r^2 + r'^2)E|v_r - v_{r'}|$, again analogous to the kinetic theory of molecules (Reif 1965, Section 12.2), but in which an efficiency E has been included to account for deviations from the hard sphere collision cross-section. Finally, when n_r droplets are considered instead of just one, the total collision rate (number of collisions per time, per volume) is $\mathcal{N}_c = n_r n_{r'}\kappa(r, r')$. The n^2 dependence, which can be seen in Equation 1 as an f^2 dependence, is a direct result of the assumption of droplets being distributed with uniform probability (i.e., the probability of finding a given number of droplets in a volume obeys the Poisson pdf).

Collision kernels can be derived for many scenarios, including Brownian motion (e.g., Seinfeld & Pandis 1998), turbulent shear flows (Saffman & Turner 1956), and gravitational sedimentation (e.g., Rogers & Yau 1989). Gravitational coalescence, where a droplet of size r falls through a quiescent fluid overtaking smaller droplets of size r', is thought to be the most effective mechanism for cloud droplets (e.g., Pruppacher & Klett 1997, Seinfeld & Pandis 1998). We note, however, that results discussed in Section 6 may lead to changes in this conclusion. For gravitational coalescence, the collision kernel grows approximately as r^6 for r between 10 and 50 μm (Pruppacher & Klett 1997, Sections 15.1, 15.2). It is clear, therefore, that the collision time $\tau(r)$ decreases extremely rapidly as r increases, making the process of collision-coalescence quite sensitive to the exact droplet size distribution $f(r)$. Furthermore, the r^6 dependence leads to a (continuous) droplet growth rate with the approximate functional dependence $dr/dt \propto r^4$, whereas the condensation growth rate varies as $dr/dt \propto r^{-1}$. So we see that there will be a transition from droplet growth dominated by condensation in the earliest stages of cloud development (small r) to growth dominated by collision and coalescence for the fraction of droplets that reach a sufficiently large radius first. An example of the resulting explosive growth when the collision-coalescence process begins is given in Figure 3.

Based on simple mass ratios (cloud droplets versus rain droplets), only approximately one in 10^6 droplets must grow large enough to initiate the

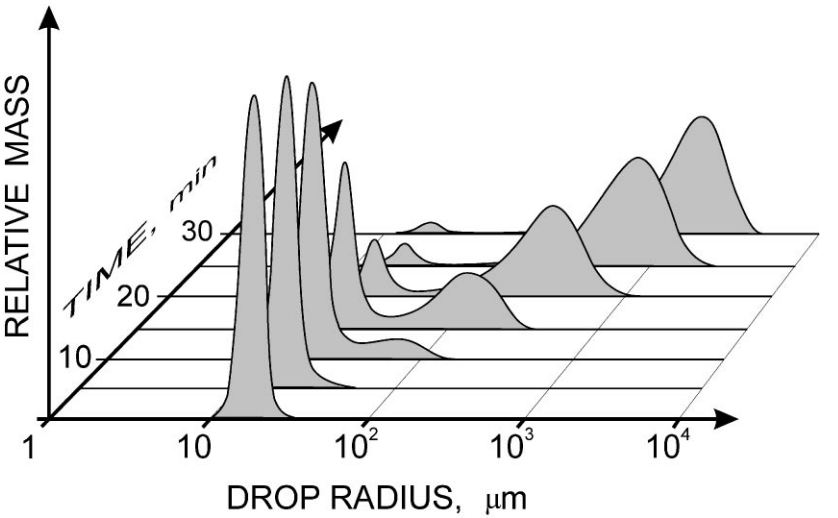

Figure 3 Illustration of the evolution of a droplet size distribution during the onset of the collision-coalescence process. Figure adapted from Berry & Reinhardt (1974) and Lamb (2001), courtesy of D. Lamb, Penn State University.

Annu. Rev. Fluid Mech. 2003.35:183-227. Downloaded from www.annualreviews.org
by Fordham University on 01/19/13. For personal use only.

collision-coalescence growth process (e.g., Rogers & Yau 1989), again accentuating the importance of understanding the details of processes that influence the droplet size distribution.

The problem of large-drop production to initiate the formation of rain has been a focal point of cloud physics research for several decades (see texts by Cotton & Anthes 1989, Pruppacher & Klett 1997, and Rogers & Yau 1989 for additional discussion). Often the discussion has been focused on the width of the droplet size distribution, with broad distributions tending to increase the gravitationally induced collision rate. This, of course, goes against the tendency of condensation growth to cause a size distribution to become narrower with time. Hence, these related concepts have driven longstanding efforts to compare calculated and measured droplet size distributions in convective clouds (e.g., see Cotton & Anthes 1989). In general, observed size distributions are significantly broader than calculated (e.g., Austin et al. 1985, Brenguier 1990, Hill & Choularton 1985). Some of the "broadening" is due to instrumental artifacts, but recent measurements suggest that there still is a discrepancy even when instrumental effects are accounted for and measurements are confined to thermodynamically isolated regions of cloud where mixing and dilution has not altered the size distribution (Brenguier & Chaumat 2001, Lasher-Trapp & Cooper 2000). Particularly interesting are the observations of "super-adiabatic" droplets, which are larger than the maximum size predicted by models of condensation growth in an isolated rising volume of cloud (e.g., Hill & Choularton 1985, Brenguier & Chaumat 2001).

3. THE NATURE OF TURBULENCE IN CLOUDS

Turbulent atmospheric flows, including convective clouds, are characterized by enormous Reynolds numbers. For example, the inertial subrange in the atmospheric boundary layer can extend from hundreds of meters to millimeters, resulting in turbulence (large-eddy) Reynolds numbers on the order of $R_t \sim 10^7$. An additional characteristic of atmospheric turbulence is the strong intermittency of certain quantities, such as energy dissipation and scalar variance, on small spatial scales (e.g., Sreenivasan & Antonia 1997, Warhaft 2000, Wyngaard 1992). The nature of atmospheric turbulence at fine scales and its interactions with other processes, such as cloud development, are areas of active research (Muschinski & Lenschow 2001). While recognizing that other mechanisms likely contribute to this broadening (e.g., Feingold & Chuang 2002), here we focus on the possible roles of fine-scale turbulence.

The main sources of turbulent kinetic energy in clouds are shear evaporative cooling due to entrainment of dry air (mostly at cloud top) and heating due to condensation growth (mostly at cloud base) (Cotton & Anthes 1989, Pruppacher & Klett 1997, Smith & Jonas 1995). The kinetic-energy dissipation rate ϵ varies by several orders of magnitude in turbulent clouds; $\epsilon \sim 10^{-2}$ m^2 s^{-3} is a typical value for moderate cumulus convection (e.g., Pruppacher & Klett 1997, Weil et al. 1993). The rms velocity also varies over at least two orders of magnitude, and for moderate cumulus convection $u_{rms} \sim 1$ m s^{-1} is typical (e.g., see Figure 2). Given a typical large-eddy scale $l \sim 10^2$ m, the large-eddy Reynolds number $R_t \sim l u_{rms}/\nu \sim 10^7$. The Kolmogorov scale is on the order of $\lambda_k = (\nu^3/\epsilon)^{1/4} \sim 10^{-3}$ m, where the kinematic viscosity of air is on the order of $\nu \sim 10^{-5}$ m^2 s^{-1}. Thus, turbulence in clouds is characterized by very large Reynolds numbers, relatively small energy dissipation rates (as compared with many engineering flows), moderate rms velocities, and a large inertial subrange spanning several orders of magnitude.

3.1. Fine-Scale Intermittency

Energy dissipation in the smallest scales of turbulence is unevenly distributed in space, or intermittent, and this intermittency steadily increases with Reynolds number (Wyngaard 1992, Sreenivasan & Antonia 1997). Similar fine-scale intermittency is observed in scalar gradients (Warhaft 2000) and Lagrangian accelerations (Hill 2002, Voth et al. 1998). By intermittency, it is meant that the probability of large-amplitude fluctuations is greatly increased relative to what might be expected for a normally distributed random variable. A pdf of velocity gradients, therefore, has long, nearly exponential tails, which grow flatter with increasing Reynolds number (e.g., see Figure 1 in Wyngaard 1992). For example, the velocity gradient probability density functions of typical numerical studies of turbulence (direct numerical simulations) have a kurtosis of order 1, whereas values on the order of 10 are found in the turbulent atmosphere (e.g., Figure 6 in Sreenivasan & Antonia 1997). The strong dissipation-rate intermittency present in a turbulent flow in

Annu. Rev. Fluid Mech. 2003.35:183-227. Downloaded from www.annualreviews.org
by Fordham University on 01/19/13. For personal use only.

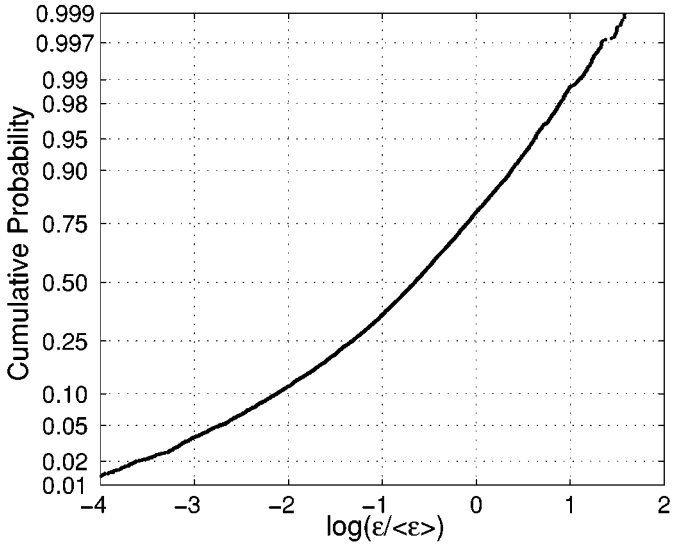

Figure 4 Cumulative probability distribution of the kinetic energy dissipation rate for a selection of velocity data obtained in a high-Reynolds-number atmospheric flow. The ordinate is $P(\log(\epsilon/\overline{\epsilon}) < x)$, stretched so that a normal distribution will lie on a straight line. Over nearly two decades around the mean, therefore, the probability distribution of $\epsilon/\overline{\epsilon}$ is approximately lognormal. This implies, for example, that dissipation rates greater than 10 times the mean occupy approximately 1% of the fluid volume. As discussed in the text, the acceleration scale corresponding to $10\overline{\epsilon}$ is roughly 2 to 40 m s^{-2} for realistic values of $\overline{\epsilon}$. Data from the FLAT90 field experiment, courtesy of S.P. Oncley, NCAR. Figure adapted from Shaw & Oncley (2001).

Annu. Rev. Fluid Mech. 2003.35:183-227. Downloaded from www.annualreviews.org
by Fordham University on 01/19/13. For personal use only.

the atmospheric boundary layer (not in the presence of clouds) is illustrated in Figure 4. Noting that the ordinate is stretched so that a lognormal function will lie on a straight line, it becomes clear why one of the earliest descriptions of a spatially varying ϵ was the lognormal model. In essence, the "landscape" of small-scale turbulence looks drastically different at high Reynolds numbers from its low-Reynolds-number counterpart.

An immediate question arises as to the relevance of intermittency to cloud processes occurring on small scales. One of the earliest considerations of this was by Tennekes & Woods (1973), who assumed that some cloud processes likely are sensitive to the rare but intense dissipation events commonly observed in atmospheric turbulence. For example, motion of cloud droplets relative to the surrounding air is caused by gravitational and Lagrangian fluid accelerations (see Section 4). The fluid-induced acceleration of cloud droplets is dominated by the smallest scales in a turbulent cloud, and the mean-square Lagrangian acceleration is a function of the average energy dissipation rate, $\langle a_L^2 \rangle = a_0 \overline{\epsilon}^{3/2} \nu^{-1/2}$ (Monin &

Annu. Rev. Fluid Mech. 2003.35:183-227. Downloaded from www.annualreviews.org
by Fordham University on 01/19/13. For personal use only.

Yaglom 1975, Section 21.5). For $a_o \approx 10$, as estimated by Voth et al. (1998) in recent laboratory studies at high Reynolds numbers, and $\overline{\epsilon} \sim 10^{-2}$ m^2 s^{-3}, the rms Lagrangian acceleration is $a_{L,rms} \sim 2$ m s^{-2}. The mean fluid acceleration, therefore, might be considered negligible when compared with the gravitational acceleration g. In atmospheric turbulence, however, where 1% of the fluid volume may correspond to dissipation rates greater than $10\overline{\epsilon}$ (see Figure 4), we would expect local Lagrangian accelerations to be of the same order as or greater than the gravitational acceleration.

Modifications to account for intermittency must be made when using relationships based on Kolmogorov scaling. For example, Hill & Wilczak (1995) and Hill (2002) point out that the scaling law $\langle a_L^2 \rangle = a_o \overline{\epsilon}^{3/2} \nu^{-1/2}$ must be modified at large Reynolds numbers to account for increasing intermittency. In essence, the relationship $\langle a_L^2 \rangle = a_o \overline{\epsilon}^{3/2} \nu^{-1/2}$ is based on the assumption of Gaussian-distributed velocity gradients, which implies that the rms acceleration is underestimated at large Reynolds numbers. Hill & Wilczak (1995) provide a means for estimating the mean-square Lagrangian acceleration from single-component measurements of velocity, such as hot-wire data from the atmospheric boundary layer:

$$\langle a_L^2 \rangle = 4H_\chi \int_0^\infty \langle (u - u')^4 \rangle \mathrm{r}^{-3}\, d\mathrm{r}, \tag{6}$$

where $\langle (u - u')^4 \rangle$ is a fourth-order velocity structure function, r is the lag between primed and unprimed velocities (Hill & Wilczak 1995, Equation 48), and H_χ is a constant that has been evaluated in numerical simulations. Shaw & Oncley (2001) calculated the fourth-order velocity structure function from the data used to generate Figure 4 and used Equation 6 to calculate an rms Lagrangian acceleration of 19 m s^{-2}. They found that this result was consistent with the scaling recently proposed by Hill (2002) that $\langle a_L^2 \rangle \propto \overline{\epsilon}^{3/2} \nu^{-1/2} \mathrm{R}_\lambda^{1/4}$. Hill's theory and these calculations suggest that rms Lagrangian accelerations can be several times larger than the gravitational acceleration for realistic atmospheric Reynolds numbers. Indeed, recent laboratory studies have revealed intense Lagrangian accelerations in turbulent flows (Hill & Thoroddsen 1997, La Porta et al. 2001, Voth et al. 1998), and other evidence exists for their presence in the atmosphere as well (Shaw & Oncley 2001).

Another aspect of fine-scale intermittency that may prove useful to understanding the nature of fluid-particle interactions is the possible link to long-lived vortex structures. For example, in their pioneering study, Tennekes & Woods (1973) concluded that further progress in understanding cloud particle–turbulence interactions would depend on finding a "definition of dissipative filaments in the microstructure of turbulence." At that time there was speculation that vortex tubes might be related to fine-scale intermittency. More recently, improvements in computational and laboratory capabilities have allowed for the detailed study of small-scale turbulence and vortex tubes over a broad range of Reynolds numbers, from $\mathrm{R}_t \sim 10^3$–10^6 (e.g., Belin et al. 1997, Cadot et al. 1995, Dernoncourt et al. 1998, Jiménez et al. 1993, Schwartz 1990, She et al. 1990). Many of these studies have

concentrated on the three-dimensional properties of vortex tubes by visualization of numerically produced vorticity fields or by laboratory techniques such as bubble migration and ultrasound. The largest Reynolds numbers in which vortex tubes have been studied have approached values typically encountered in the atmosphere ($R_t \sim 10^6$ to 10^8). These studies provide a picture of small-scale turbulence consisting of intense regions of vorticity organized in cylindrical structures referred to as tubes, worms, or filaments. Their lifetime and intensity appear to be directly tied to the largest scales in the turbulence, whereas their diameters are between the Kolmogorov and Taylor microscales. The size, volume fraction, lifetime, and intensity of these vortex tubes all depend on the turbulence Reynolds number.

A final aspect of cloud turbulence that is crucial to understanding precipitation development and cloud evolution is the entrainment and mixing of dry air from the surrounding environment into a cloud. The broad topic of entrainment has been reviewed by Blyth (1993). Qualitatively, much can be learned about the entrainment process by considering a horizontal traverse through a cloud, such as that shown in Figure 2. One of the striking features that is confirmed by our own day-to-day observations of clouds is the sharpness of cloud boundaries. The nongradient mixing model by Broadwell & Breidenthal (1982), which provides a physically based mechanism for the formation of extremely sharp boundaries in scalar concentration, is considered to be representative of the mixing process in clouds (e.g., Baker et al. 1984, Gerber 1991). Of course, cloud droplets are not just passive tracers; they are finite-sized particles with inertia, and they interact thermodynamically with their environment, leading to processes such as buoyancy reversal that tend to enhance fine-scale intermittency (e.g., Grabowski 1993). As cloud droplets are successively exposed to regions of enhanced and depleted water vapor concentration because of mixing, and as other complex interactions between mixing, sedimentation, and vertical velocities occur, droplet size distributions may become broader than otherwise predicted (e.g., Cooper 1989, Jensen & Baker 1989). This is of great relevance to the formation of precipitation, as discussed in Section 5.

Annu. Rev. Fluid Mech. 2003.35:183-227. Downloaded from www.annualreviews.org
by Fordham University on 01/19/13. For personal use only.

3.2. Randomness and the Pair Correlation Function

The study of turbulent flows is based on the notion that quantities such as velocity or temperature can be considered random variables. This leads to utilization of the tools of statistical physics, including correlation functions, power spectra, etc. To study the nature of turbulent clouds, similar tools are used (e.g., Davis et al. 1999, Gerber et al. 2001). When processes occurring at centimeter scales and below are considered, however, the discreteness of cloud droplets must be noted (e.g., Baker 1992, Chaumat & Brenguier 2001, Kostinski & Shaw 2001). Here we provide a brief overview of several concepts that allow the discrete, but still random, nature of the spatial distribution of cloud droplets to be quantified using the language of counting processes.

Most processes occurring in clouds, such as condensation growth (e.g., Srivastava 1989, Vaillancourt et al. 2002), collision-coalescence (e.g., Pinsky &

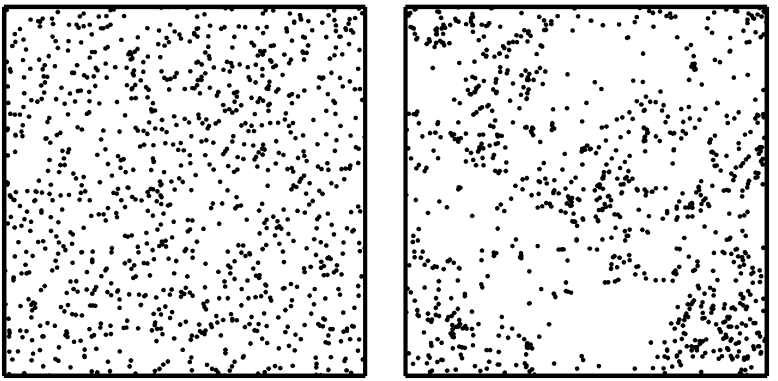

Figure 5 Two examples of 1000 particles with spatial positions in two dimensions chosen randomly. *Left panel*: Statistically homogeneous Poisson process. Particle positions are uniformly and independently distributed random variables. This is the perfect randomness standard for dilute systems of particles. *Right panel*: Statistically homogeneous but spatially correlated (not Poisson) random process. Particle positions are uniformly distributed but not independent random variables.

Annu. Rev. Fluid Mech. 2003.35:183-227. Downloaded from www.annualreviews.org
by Fordham University on 01/19/13. For personal use only.

Khain 1997a), and the propagation of electromagnetic radiation (e.g., Kostinski 2001, Marshak et al. 1998), are linked to the spatial and temporal distribution of cloud droplets. Of course, this requires that we account for the apparent randomness of the small-scale features of clouds. For example, the number of cloud droplets in a volume can be considered a random but countable variable. Figure 5 is a cartoon illustrating this notion of randomness, both with and without spatial correlations. The left panel represents perfect randomness for a collection of droplets. It is referred to as perfect because particle positions are uniformly distributed and statistically independent (uncorrelated), and the process is statistically homogeneous (e.g., Shaw et al. 2002b). These conditions define a Poisson process, characterized by the Poisson distribution on any scale, so that the number of particles $N(V)$ in a test volume V is distributed according to

$$p(N) = \frac{\bar{N}^N \exp(-\bar{N})}{N!}, \tag{7}$$

where $\bar{N}$ is the mean number of particles in V. It is important to note that the validity of the Poisson distribution on some spatial scale V does not imply the Poisson process. For example, positive and negative deviations from the Poisson process on smaller spatial scales can cancel each other and result in Poisson statistics on longer scales (as was shown by Kostinski & Shaw 2001). The Poisson process, or perfect randomness, implies the absence of correlations on all scales.

A statistically homogeneous but spatially correlated random process is illustrated in the right panel of Figure 5. This is not a Poisson random process because particle positions are no longer statistically independent owing to the presence of

Annu. Rev. Fluid Mech. 2003.35:183-227. Downloaded from www.annualreviews.org
by Fordham University on 01/19/13. For personal use only.

clusters and voids. The clustering is quantified by the pair correlation function η, specifically defined as a deviation from perfect randomness (see Equation 8). It should be noted that the statistically homogeneous random process illustrated in the right panel of Figure 5 is fundamentally different from a statistically inhomogeneous Poisson process, where the mean particle density is spatially dependent and deterministic [e.g., an ideal gas of molecules in a gravitational field, where $\overline{n}$, is a deterministic function of height (Shaw et al. 2002b)]. However, at sufficiently small scales (e.g., sub-grid scales in a large-eddy simulation of a cloud) the local number density of cloud particles is not a predictable function. Although the assumption often is implicit, typically the homogeneous uncorrelated approach (Poisson process) is used at these scales, as, for example, in the theory of collision and coalescence of cloud droplets [e.g., Pruppacher & Klett (1997); also see Section 2]. However, in the presence of turbulent mixing, or when droplet inertia is accounted for, correlations will exist, so we must use the homogeneous but correlated random process approach. This serves as motivation for quantifying correlations in droplet positions as a function of spatial scale. Which scales are relevant to a particular problem will depend on the physical process under consideration.

Positive spatial correlations, such as in the right panel of Figure 5, result in clustering at some range of spatial scales. In contrast, when negatively correlated (e.g., particle repulsion), the resulting particle distribution is more uniform than perfect randomness at that length scale. To quantify this picture, we consider a volume element dV sufficiently small so that it can contain only one droplet, and so that the probability of finding a droplet in that volume is $\overline{n}dV$, where $\overline{n}$ is the mean droplet number density. If droplet positions are uncorrelated, then we would expect that the conditional probability of finding a droplet in volume element dV separated by distance r from a reference drop is $P_{1,2}(\mathrm{r}) = \overline{n}dV$ (noting that the symbol r implies isotropy). If, however, the positions are correlated we define the pair correlation function $\eta(\mathrm{r})$ as

$$P_{1,2}(\mathrm{r}) = \overline{n}dV[1 + \eta(\mathrm{r})] \tag{8}$$

(Landau & Lifshitz 1980). The pair correlation function is zero for perfect randomness and has a lower limit of -1, e.g., for scales less than the diameter of impenetrable particles. If the pair correlation function is greater than zero, it implies that when a droplet is encountered at a given position in a cloud, there is an enhanced probability of finding another droplet distance r away. It should also be mentioned that in the fluid mechanics literature the pair correlation function often is referred to as the radial distribution function $g(\mathrm{r}) = \eta(\mathrm{r}) + 1$ (e.g., Reade & Collins 2000, Sundaram & Collins 1997, Wang et al. 2000).

It follows from Equation 8 that $\eta(\mathrm{r})$ can be written in the form (Kostinski & Jameson 2000, Shaw et al. 2002b)

$$\eta(\mathrm{r}) = \frac{\overline{N(\mathrm{r_o})N(\mathrm{r_o} + \mathrm{r})}}{\overline{N}^2} - 1, \tag{9}$$

which we may take as an operational definition. This is a powerful result because it provides a direct, albeit subtle, link to the traditional autocorrelation function $\rho(\mathrm{r})$

defined for continuous random variables. Neglecting r = 0, the two are related via

$$\eta(\mathrm{r}) = \rho(\mathrm{r})\frac{\overline{n'^2}}{\overline{n}^2}, \tag{10}$$

where $n' \equiv n - \overline{n}$ is the fluctuating component (Shaw et al. 2002b). As with $\rho(\mathrm{r})$, $\eta(\mathrm{r}) \to 0$ as $\mathrm{r} \to \infty$, but as $\mathrm{r} \to 0$, the pair correlation function is not confined to approach unity. This will be of some consequence when the pair correlation function is introduced to the theory of collision and coalescence where correlations on the scale of a droplet radius are considered.

Annu. Rev. Fluid Mech. 2003.35:183-227. Downloaded from www.annualreviews.org
by Fordham University on 01/19/13. For personal use only.

4. DROPLET MOTION IN TURBULENCE

Fundamental to understanding the influence of turbulence on cloud processes is the motion of an individual cloud droplet. In many basic treatments of cloud processes, droplets are assumed to move with a steady-state fall velocity v_T, but this neglects the contribution of fluid accelerations, which under some flow conditions are of the same order or larger than the gravitational acceleration g. For small cloud droplets, the Reynolds number typically is sufficiently small so that the Stokes drag force is a reasonable approximation. In this limit, Newton's second law for a sphere with velocity $\mathbf{v}$ in a viscous fluid with uniform (but time varying) velocity $\mathbf{u}$ is

$$\rho_d V_d \frac{d\mathbf{v}}{dt} = 6\pi\mu r\,(\mathbf{u}-\mathbf{v}) + \frac{1}{2}\rho_f V_d\,(\dot{\mathbf{u}}-\dot{\mathbf{v}}) + 6r^2\sqrt{\pi\rho_f\mu}\int_0^t \frac{\dot{\mathbf{u}}(t')-\dot{\mathbf{v}}(t')}{\sqrt{t-t'}}dt' + \rho_d V_d\mathbf{g} + \rho_f V_d\,(\dot{\mathbf{u}}-\mathbf{g})\,. \tag{11}$$

Here, μ and ρ_f are the dynamic viscosity and density of the surrounding fluid (air), ρ_d is the density of the droplet (water), and $V_d = 4/3\pi r^3$ is the droplet volume. The terms on the right of Equation 11 are, in order, the Stokes drag force, the "added mass" force due to acceleration of the surrounding fluid, the Basset "history" force due to diffusion of vorticity from an accelerating particle, the gravitational force, and finally, two terms resulting from the stress field of the fluid flow acting on the particle (including a shear stress term and a pressure gradient or buoyancy term). More thorough discussions of the equation of motion for a sphere are available in the literature (e.g., Corrsin & Lumley 1956, Manton 1977, Maxey & Riley 1983). For the sake of brevity, we mention only that Equation 11 is based on several limiting assumptions that typically are valid for cloud droplets, including the neglect of flow curvature, slip corrections, and interaction with boundaries or other particles. Obviously, the latter restriction must be relaxed if details of the collision-coalescence are to be considered, but in clouds the volume fraction ϕ of droplets is sufficiently small, typically on the order of $\phi = nV_d \sim 10^{-6}$, so that droplet-droplet interactions typically can be ignored for the majority of a droplet trajectory.

Annu. Rev. Fluid Mech. 2003.35:183-227. Downloaded from www.annualreviews.org
by Fordham University on 01/19/13. For personal use only.

4.1. Relative Velocity and Dimensionless Scales

To understand the origin of particle clustering in turbulent flows we are especially interested in terms that decouple the particles from the incompressible fluid, for example, any term containing a relative particle-fluid velocity. In an approximate sense, these terms allow us to consider the droplet phase as a compressible fluid, thereby making its dynamics even richer than for typical scalar quantities. Defining $\mathbf{w} \equiv \mathbf{v} - \mathbf{u}$ and dividing by droplet mass, we obtain from Equation 11

$$\frac{d\mathbf{w}}{dt} = -\frac{\mathbf{w}}{\tau_d} - \frac{\rho_f}{\rho_d}\frac{\dot{\mathbf{w}}}{2} - \left(\frac{9}{2\pi\tau_d}\frac{\rho_f}{\rho_d}\right)^{1/2}\int_0^t \frac{\dot{\mathbf{w}}(t')}{\sqrt{t-t'}}\,dt' + \left(1-\frac{\rho_f}{\rho_d}\right)\mathbf{g} - \left(1-\frac{\rho_f}{\rho_d}\right)\dot{\mathbf{u}}. \quad (12)$$

The last term on the right side represents the effect of Lagrangian fluid accelerations in generating relative droplet-fluid accelerations. Mathematically, the last two terms on the right are the only nonhomogeneous terms in the differential equation and therefore can be considered to be the external drivers of droplet motion. To estimate the magnitudes of the various terms in Equation 12, it is necessary to introduce characteristic scales τ_f and u_o for the fluid and w_o for the relative velocity. For example, relative droplet acceleration scales as $\dot{\mathbf{w}} = (w_o/\tau_f)\dot{\mathbf{w}}^*$, and fluid acceleration scales as $\dot{\mathbf{u}} = (u_o/\tau_f)\dot{\mathbf{u}}^*$, where all starred variables are dimensionless. Finally, the gravitational acceleration is written as $\mathbf{g} = |\mathbf{g}|\mathbf{g}^*$. In this form, three natural dimensionless parameters arise from the equation of motion: density ratio $\alpha = \rho_f/\rho_d$, droplet Stokes number $S_d = \tau_d/\tau_f$, and acceleration ratio (Froude number) $F_f = g\tau_f/u_o$. Using these definitions, and neglecting terms of order $\alpha \sim 10^{-3}$ and smaller, Equation 12 becomes

$$\mathbf{w}^* + S_d\dot{\mathbf{w}}^* + \left(\frac{9}{2\pi}\alpha S_d\right)^{1/2}\int_0^{t^*}\frac{\dot{\mathbf{w}}^*}{\sqrt{t^*-t^{*\prime}}}dt^{*\prime} = -S_d\frac{u_o}{w_o}\left(\dot{\mathbf{u}}^* - F_f\mathbf{g}^*\right) \quad (13)$$

(e.g., Manton 1977). Usually it is assumed that the acceleration ratio $F_f \gg 1$ so that $w_o = \tau_d g$ and Equation 13 reduces to $\mathbf{w}^* + S_d\dot{\mathbf{w}}^* = \mathbf{g}^*$. In dimensional form, this has the solution $w = \tau_d g(1 - \exp(-t/\tau_d))$ and represents a simple relaxation of relative velocity to the terminal fall speed. It has been pointed out, however, that even in moderately turbulent clouds the Lagrangian fluid acceleration $\dot{\mathbf{u}}$ can be of the same order of magnitude as $\mathbf{g}$ and that in localized regions within a turbulent flow it is possible to have $\dot{\mathbf{u}} \gg \mathbf{g}$ (La Porta et al. 2001, Shaw & Oncley 2001). As a result, the full equation (Equation 12 or Equation 13) must be used. The nature of fluid accelerations in turbulence is discussed at greater length in Section 3.

Clearly, much of the physics of droplet motion in a turbulent cloud is contained in the Stokes number S_d and the acceleration ratio F_f, leaving the task of estimating these parameters for realistic cloud conditions. Here we are interested especially in the nature of droplet motion during early stages of cloud formation and the

Annu. Rev. Fluid Mech. 2003.35:183-227. Downloaded from www.annualreviews.org
by Fordham University on 01/19/13. For personal use only.

onset of the collision and coalescence process. Therefore, we take $r \sim 10\ \mu$m as a droplet radius scale. To obtain appropriate fluid time and velocity scales, we must consider the spatial scale in the fluid turbulence at which Lagrangian accelerations are dominant. Based on the traditional picture of the turbulent cascade, scaling arguments suggest that Lagrangian accelerations scale as $a_l \sim \epsilon^{2/3} l^{-1/3}$, where l is the eddy length scale and ϵ is the kinetic energy dissipation rate per unit mass (Monin & Yaglom 1975, Section 21.5). Thus, Lagrangian accelerations are dominant at the smallest spatial scales of the flow, corresponding to the dissipation or Kolmogorov scale λ_k. Because it is assumed that properties of the dissipation-scale eddies depend only on ν and ϵ, it follows that these eddies will have a timescale $\tau_k = (\nu/\epsilon)^{1/2}$. Therefore the Stokes number for droplets in a turbulent flow is

$$\mathrm{S}_d = \frac{\tau_d}{\tau_k} = \frac{2\rho_d \epsilon^{1/2} r^2}{9\rho_f \nu^{3/2}}. \tag{14}$$

For typical cloud conditions ($\epsilon \sim 10^{-2}$ m^2 s^{-3}, $\nu \sim 10^{-5}$ m^2 s^{-1}) and $r \sim 10^{-5}$ m, the Stokes number is close to the order $S_d \sim 10^{-1}$. An example of the distribution of particles resulting from a direct numerical simulation of homogeneous, isotropic turbulence containing cloud droplets (with realistic Stokes number and energy dissipation rate; see Vaillancourt et al. 2002) is shown in Figure 6, to be discussed in greater detail in Section 5. For now, we note the tendency for cloud droplets to

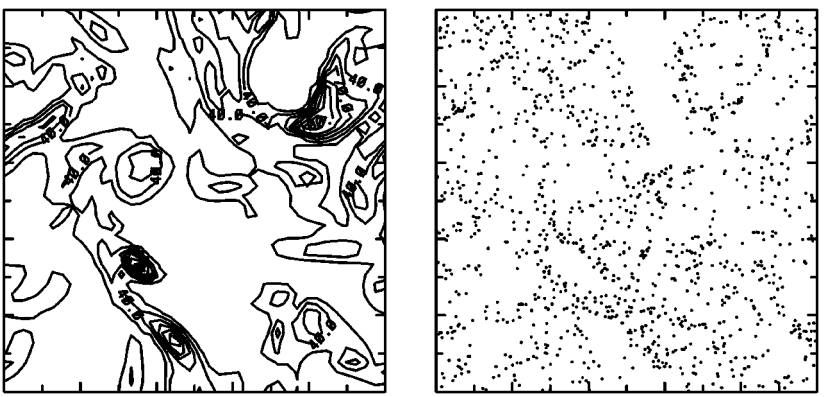

Figure 6 A slice through the computational domain of a direct numerical simulation of homogeneous, isotropic turbulence containing particles. The gravitational acceleration, particle Stokes number, kinetic energy dissipation rate, and Kolmogorov scales are matched to those typically encountered in an atmospheric cloud. Given these scales, the slice is 0.1 m on a side. The *left panel* shows vorticity contours, and the *right panel* shows droplet positions, illustrating the tendency of droplets to form clusters in regions of low vorticity. Figure adapted from Vaillancourt et al. (2002), courtesy of P. Vaillancourt, Meteorological Service of Canada.

form clusters in regions of low vorticity owing to their finite inertia. The equation of motion for the droplets includes Stokes drag and gravitational acceleration, but does not include the history term (Vaillancourt et al. 2001). Of course, this type of numerical simulation is unable to approach the large turbulence Reynolds numbers that exist in the atmosphere and, as a result, the local variation in the acceleration ratio is expected to be much smaller than in the atmosphere.

The history term is difficult to compare with other terms because the integral depends on the specific flow and droplet path under consideration. However, it is retained in Equation 13 because it scales as $\alpha^{1/2}$ and $S_d^{1/2}$ and therefore, for flows with large fluid accelerations, the history term can be important (e.g., Corrsin & Lumley 1956, Manton 1974; R.J. Hill, personal communication). As Fuchs (1989) aptly puts it, the history term is "neglected in most published work on aerosols, no arguments to justify the simplification having been put forward." The presence of strong acceleration intermittency in atmospheric turbulence (e.g., Hill 2002, La Porta et al. 2001, Shaw & Oncley 2001, Voth et al. 1998) suggests that, in addition to the other terms, it will likely be necessary to consider the role of the history term in cloud-droplet motion more carefully in future research.

Annu. Rev. Fluid Mech. 2003.35:183-227. Downloaded from www.annualreviews.org
by Fordham University on 01/19/13. For personal use only.

4.2. Droplet Inertia and Number Density Fluctuations

Droplet growth both by condensation and by collision-coalescence is influenced directly by the local number density n of cloud droplets. It is of interest, therefore, to consider fluctuations in n, including possible temporal and spatial correlations. For the sake of transparency, we use the simplified droplet equation of motion

$$\frac{d\mathbf{v}}{dt} = \frac{1}{\tau_d}(\mathbf{u} - \mathbf{v}) + \mathbf{g}. \tag{15}$$

In the limit of small τ (small particle inertia), which is satisfied during the early stages of cloud development, Equation 15 has the approximate solution

$$\mathbf{v} = \mathbf{u} + \tau_d \mathbf{g} - \tau_d \dot{\mathbf{u}} + \mathcal{O}\left(\tau_d^2\right), \tag{16}$$

which has the reasonable physical interpretation that, for example, droplets will lag the fluid when the fluid experiences a positive local acceleration. It is crucial to make special note here that $\dot{\mathbf{u}}$ is the *total* acceleration, $\dot{\mathbf{u}} = \partial\mathbf{u}/\partial t + \mathbf{u}\cdot\nabla\mathbf{u}$. Number density fluctuations are a manifestation of compressibility of the particle phase, as can be seen from the conservation equation for droplet number density,

$$\frac{dn}{dt} = \frac{\partial n}{\partial t} + \mathbf{v}\cdot\nabla n = -n\nabla\cdot\mathbf{v}. \tag{17}$$

We proceed, therefore, by calculating the divergence of the droplet velocity from Equation 16:

$$\nabla\cdot\mathbf{v} = -\tau_d\nabla\cdot(\mathbf{u}\cdot\nabla\mathbf{u}) = -\tau_d\left(\frac{\partial u_i}{\partial x_j}\right)\left(\frac{\partial u_j}{\partial x_i}\right), \tag{18}$$

Annu. Rev. Fluid Mech. 2003.35:183-227. Downloaded from www.annualreviews.org
by Fordham University on 01/19/13. For personal use only.

where standard index notation is used in the last expression. In obtaining Equation 18, we have assumed that the surrounding fluid is incompressible so that $\nabla \cdot \mathbf{u} = 0$, and we also note that the gravitational acceleration does not contribute to the compressibility of the droplet phase. Equation 18 is Equation 5.10 of Maxey (1987), a remarkable result that has served as the basis for important subsequent work applied to cloud physics (e.g. Balkovsky et al. 2001, Elperin et al. 1996, Pinsky & Khain 1997a). Using the definitions of the strain rate tensor e_{ij} and the rotation tensor r_{ij}, one physical interpretation of Equation 18 can be made clearer by writing it in the form $\nabla \cdot \mathbf{v} = -(\tau_d/4)(4e_{ij}e_{ij} - r_{ij}r_{ij})$. The droplet velocity field is divergent for large vorticity and is convergent for large strain rate. Maxey's conclusion that "particles will tend to accumulate in regions of high strain rate or low vorticity" follows directly.

Once it is accepted that particles/droplets can be considered from the viewpoint of a continuous, compressible scalar constituent (i.e., Equation 17), it follows that the scalar statistics will be of interest. To this end, Elperin et al. (1996, 1998, 2000) used a path integral approach to obtain an equation for the high-order correlation function. They conclude that the particle spatial distribution is strongly intermittent when particle inertia is sufficiently large so that $\nabla \cdot \mathbf{v} \neq 0$, and also that, for cloud particles and typical turbulence scales in the atmosphere, the strongest fluctuations will occur on millimeter scales. Jeffery (2000, 2001b) has extended the correlation function for the viscous-convective subrange to obtain the spectral density of inertial particles, thereby allowing the scale dependence of density fluctuations to be investigated directly (discussed at greater length in Section 7.2). Jeffery (2000) concluded that particle inertia results in enhanced variance of the scalar dissipation rate in the viscous-convective subrange for droplet Stokes numbers larger than $S_d \approx 0.2$. This conclusion is based on the Gaussian hypothesis used by Pinsky et al. (1999a) to obtain an expression for $\langle(\nabla \cdot \mathbf{v})^2\rangle$ that effectively relates it to the droplet Stokes number (Jeffery 2000). As pointed out by Jeffery (2001b), the Gaussian hypothesis fails to account for velocity gradient intermittency that exists at large Reynolds numbers. To account for these effects, Jeffery (2001b) shows that $\langle(\nabla \cdot \mathbf{v})^2\rangle$ can be related to three scalar invariants that are functions of kinetic energy dissipation rate and enstrophy. Assuming that the dissipation rate term is dominant, he incorporates the Reynolds number dependence into an effective Stokes number proportional to the square root of the longitudinal velocity gradient flatness factor. Jeffery estimates that in the atmospheric boundary layer the effective Stokes number is approximately $2.7S_d$.

Finally, we note that direct numerical simulations of isotropic turbulence containing particles also have shown that significant number density fluctuations arise for particles for a range of particle Stokes numbers (e.g., Eaton & Fessler 1994, Hogan et al. 1999, Reade & Collins 2000, Sundaram & Collins 1997, Wang et al. 2000). In many of these studies the phenomenon has been referred to as "preferential concentration," descriptive of the remarkable "unmixing" of particles in turbulence due to their finite inertia. A full review of this work is not possible here, but briefly, the results generally confirm that particles with Stokes numbers on

the order of 1 tend to drift to regions of low vorticity. Qualitatively, particles with very small Stokes numbers tend to follow fluid streamlines, and particles with very large Stokes numbers do not respond to the fluid significantly during the lifetime of an eddy. Therefore, particles with Stokes numbers near 1 are effectively resonant with dissipation-scale eddies in turbulent flow.

5. DROPLET GROWTH BY CONDENSATION

As discussed in Section 2, the standard theory of droplet growth by condensation in a closed parcel results in narrow droplet size distributions. This is in contrast to many observations of droplet distributions in clouds, even in core regions where entrainment of dry air is nonexistent or weak. Especially compelling is the possible presence of super-adiabatic drops that are larger than can be explained even for a completely undiluted cloud (e.g., Brenguier & Chaumat 2001, Hill & Choularton 1985) because they may serve to initiate the collision-coalescence process.

Annu. Rev. Fluid Mech. 2003.35:183-227. Downloaded from www.annualreviews.org
by Fordham University on 01/19/13. For personal use only.

5.1. Stochastic Condensation

One approach for including condensation in a turbulent flow is to perform Reynolds averaging on the equation for condensation growth, resulting in covariances that can be thought of as "Reynolds stresses." We cover this approach in detail because it provides a direct link to standard turbulence techniques and it reveals some of the underlying difficulties in describing condensation growth in a turbulent flow. To begin, we consider just the condensation portion of Equation 1, $\partial f(r)/\partial t = \partial[\dot{r} f(r)]/\partial r$. Following the standard approach for Reynolds averaging, with variables consisting of mean and fluctuating components $f = \bar{f} + f'$ and $\dot{r} = \bar{\dot{r}} + \dot{r}'$, we have

$$\frac{d\bar{f}}{dt} = -\frac{\partial(\bar{\dot{r}}\,\bar{f})}{\partial r} - \frac{\partial(\overline{\dot{r}' f'})}{\partial r}. \tag{19}$$

This is known as the stochastic condensation equation, and there is a large amount of literature devoted to its formulation, and to obtaining solutions for various limits (e.g., Stepanov 1975; Pruppacher & Klett 1997, Chapter 13). In most cases, Equation 19 is solved under the assumption that turbulent fluctuations in the supersaturation field are much slower than the phase relaxation time τ_s (see Equation 3). In fact, we may borrow terminology from the field of reactive flows (e.g., Libby & Williams 1980) and define a supersaturation Damköhler number, $\mathrm{D}_s = \tau_f/\tau_s$, where τ_f is a fluid timescale. In what has been called the low frequency limit, we have $\mathrm{D}_s \gg 1$ and may expect strong interactions between turbulence and the reactive species, in this case water vapor supersaturation.

In the covariance terms in Equation 19, f' often is obtained using simple Prandtl mixing length arguments. Fluctuations in $\dot{r}$ are often obtained by assuming that turbulent fluctuations are slow compared to the phase relaxation time τ_s, so that the

quasi-steady supersaturation can be used (see Section 2). Specifically, Equation 2 for the fluctuating component becomes $\dot{r}' = \gamma s'/r$, with $s' = \varphi u_z' \tau_s$. The key point is that both mean and fluctuating supersaturations are tied to the vertical velocity. It has been shown that this places a severe restriction on the degree to which turbulent fluctuations can lead to broadening of the size distribution (e.g., Pruppacher & Klett 1997). By allowing for vertical velocity fluctuations at cloud base and for entrainment of dry air, more recent stochastic-condensation models are able to overcome these limitations (e.g., Cooper 1989) and lead to improved agreement with observations (Politovich 1993).

It is important to consider when the low frequency limit (or large Damköhler number limit) ceases to be valid. We can estimate the spatial scale at which $D_s \sim 1$ by using Kolmogorov scaling, so that at any scale r the energy dissipation rate may be written as $\epsilon \sim u_r^3/r \sim r^2/\tau_r^3$. When $D_s = 1$, we have $\tau_s = \tau_r$, where the fluid timescale τ_f has been replaced by the scale-dependent fluid timescale τ_r. Therefore, the scale at which $D_s = 1$ can be estimated as $r^* \sim (\epsilon \tau_s^3)^{1/2}$, which for typical cloud conditions with $\tau_s \sim 10$ s, is on the order of several meters. We note that this spatial scale compares well to the observed onset of a regime of enhanced variance in liquid water content variance in clouds (see Figure 7) (also see Mazin 1999 for similar arguments). It is clear, therefore, that the low frequency limit (or large Damköhler number limit) often is not satisfied in clouds, where significant fluctuations in vertical velocity and droplet number density occur on smaller spatial scales. A recent contribution by Khvorostyanov & Curry (1999a,b) lays out a procedure for solving the stochastic collection equation for more realistic conditions where turbulent fluctuations can be of the same order as τ_s. Although simplifying assumptions are made, they are able to obtain analytical solutions for the droplet distributions in the form of gamma distributions. This is an attractive result, as many observed cloud-droplet distributions can be fitted with gamma distributions (e.g., Pruppacher & Klett 1997).

In a somewhat different approach, Kulmala et al. (1997) have developed an approach to stochastic condensation by considering mean and fluctuating components of water vapor pressure $p_v = \overline{p_v} + p_v'$ and temperature $T = \bar{T} + T'$ so that $s = (\overline{p_v} + p_v')/(p_v^*(\bar{T} + T'))$. The latter expression is expanded to second order, and the Clausius-Clapeyron equation is used to evaluate derivatives of the equilibrium vapor pressure with respect to temperature. Finally, approximate expressions for the mean and variance of the saturation ratio are obtained, which then are used in the framework of a condensation growth model. Two compelling results of this model are the activation of cloud droplets even when the mean supersaturation is negative, and the importance of supersaturation fluctuations in the overall droplet growth rate.

5.2. Droplet Number Density Fluctuations

Fluctuations in droplet number density due to finite droplet inertia and their influence on the condensation growth process have been considered by Grabowski

Annu. Rev. Fluid Mech. 2003.35:183-227. Downloaded from www.annualreviews.org
by Fordham University on 01/19/13. For personal use only.

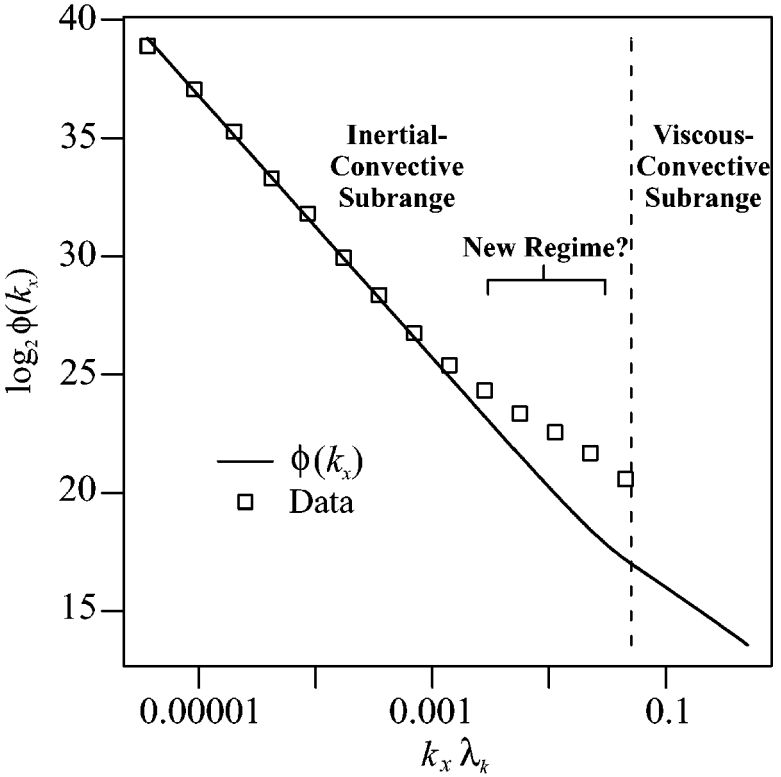

Figure 7 The one-dimensional scalar spectrum for liquid water content data obtained during the SOCEX field experiment and first presented by Marshak et al. (1998), shown as *open squares*. The observed spectrum is an order of magnitude larger than the typical inertial-convective and viscous-convective scaling, which is shown by the *solid line*. Note that the Kolmogorov length scale is on the order of 1 mm. Adapted from Jeffery (2001b), courtesy of C. Jeffery, Los Alamos National Laboratory.

Annu. Rev. Fluid Mech. 2003.35:183-227. Downloaded from www.annualreviews.org
by Fordham University on 01/19/13. For personal use only.

& Vaillancourt (1999), Jeffery (2001b), Pinsky & Khain (1997b), Pinsky et al. (1999a), Shaw et al. (1998, 1999), Shaw (2000), Vaillancourt & Yau (2000), and Vaillancourt et al. (2002). We begin a brief review of the general results by pointing out the pioneering efforts by Srivastava (1989) toward understanding the role of number density fluctuations, which exist even when no inertia is present, in the condensation process. Srivastava considered the possible effect of local number density fluctuations in a perfectly random arrangement of droplets (the number of droplets in a given volume obeying the Poisson pdf). In essence, because the local supersaturation is inversely proportional to the local number density of droplets and because of thermodynamic interactions between closely spaced droplets, this approach suggested that density fluctuations will lead to broadening of the size

distribution. Vaillancourt et al. (2001) have performed careful simulations of the condensation process for populations of droplets distributed in space with uniform probability (perfectly random). They find that significant supersaturation fluctuations are formed, but that the dispersion in droplet growth is greatly reduced when droplet sedimentation is accounted for. They conclude that the broadening of the size distribution is insufficient to match observations from unmixed cloud cores.

Vaillancourt et al. (2002) have performed the first direct numerical simulation of a turbulent flow, coupled with the droplet-condensation growth process, for parameters matched to those typically found in atmospheric clouds. A "snapshot" of vorticity (left panel) and droplet location (right panel) from their simulations is shown in Figure 6 and illustrates the tendency of droplets to cluster in regions of low vorticity. Vaillancourt et al. (2002) found the condensation process in turbulent clouds to be surprisingly complex, with droplet sedimentation, droplet inertia, and fluid mixing all playing important roles. For example, under typical conditions for a cumulus cloud there were significant number density fluctuations caused by finite particle inertia, but at the same time gravitational sedimentation tended to suppress these fluctuations. A major finding was that, although preferential concentration led to larger supersaturation fluctuations, droplet size distributions were more narrow than without the turbulence. The narrowing occurs because droplet growth rate is a function of the time integral of supersaturation and droplet inertia results in a decreased decorrelation time between droplets and their thermodynamic environment. This intriguing conclusion is in contrast to the majority of previous studies in which turbulence has led to broader size distributions.

For example, using a model of droplet number density fluctuations in Batchelor turbulence, Pinsky et al. (1999a) investigated the effects of droplet inertia on the condensation growth process. They showed that the timescale for inertial mixing of droplets between clusters at small scales is of the same order as the timescales for molecular diffusion and droplet growth. This inertial mixing and subsequent thermodynamic response led to slight broadening of the droplet size distribution. As expected, the size distributions were found to be much broader when mixing of dry air into the cloud was accounted for. In the latter case, the inertial mixing tended to produce more spatially uniform size distributions than when droplet inertia was not accounted for.

Shaw et al. (1998) investigated the Reynolds-number dependence and the effects of intermittency on the condensation growth process by using a model of droplet motion in intense, relatively long-lived vortex tubes (see Section 3). Because these structures have diameters somewhere between the Kolmogorov and Taylor microscales and peak azimuthal velocities that scale with the large-eddy velocity scale, droplets contained therein experience very large radial accelerations. This leads to an exponentially decreasing number density of droplets within a vortex, with a time constant proportional to $(r^2\epsilon)^{-1}$ (Shaw 2000). Because these intense vortex tubes persist for times on the order of the large-eddy timescale, the density fluctuations are sufficiently long lived so as to lead to large supersaturation fluctuations: Accounting for molecular diffusion, Shaw (2000) found that supersaturations

Annu. Rev. Fluid Mech. 2003.35:183-227. Downloaded from www.annualreviews.org
by Fordham University on 01/19/13. For personal use only.

larger than 10% can be reached in vortex cores. Shaw et al. (1998) used their model of droplet motion coupled with relevant thermodynamic fields and condensation growth, and concluded that significant broadening of the size distribution would occur. In a comment on this work, Grabowski & Vaillancourt (1999) argued that the presence of gravitational sedimentation will tend to reduce the effect and that the droplet Stokes numbers in clouds are too small to yield significant number density fluctuations. Shaw et al. (1999) responded that neglecting gravity is acceptable for droplet motion in a vortex because the fluid acceleration is large relative to the gravitational acceleration. They also noted that the Reynolds number dependence of fine-scale turbulence will lead to stronger density fluctuations and a broader range of Stokes numbers susceptible to preferential concentration. As discussed in Section 4.2, Jeffery (2001b) has confirmed that at very large Reynolds numbers an effective Stokes number should be used, which leads to enhanced density fluctuations. However, Jeffery argues against the statistical significance of vortex tubes in generating density fluctuations. Clearly, further work is required to clarify the role of coherent vortex structures in cloud processes.

Annu. Rev. Fluid Mech. 2003.35:183-227. Downloaded from www.annualreviews.org
by Fordham University on 01/19/13. For personal use only.

5.3. Entrainment and Mixing

The role of entrainment and mixing in cloud-droplet growth has received attention for many years and a complete treatment of the subject is beyond the scope of this review. For example, the extensive discussions of homogeneous and inhomogeneous mixing and and their role in producing large drops and bimodal size distributions, although of relevance, are not discussed here. We proceed by highlighting some recent results that are related directly to fine-scale turbulence, and refer to the review by Blyth (1993) for further details.

An aspect of mixing that has been the subject of recent research is the formation of supersaturation fluctuations by isobaric mixing (e.g., Gerber 1991, Korolev & Isaac 2000). When two parcels with different T and p_v are thoroughly mixed, the resulting temperature and vapor pressures are simple averages of the initial T and p_v weighted by volume fraction. However, the equilibrium vapor pressure $p_v^*(T)$ is a nonlinear function of T, so it does not vary linearly with volume fraction. For example, if two saturated parcels at different temperatures are mixed thoroughly, the resulting mixture will be supersaturated. Gerber (1991) used this concept in the context of nongradient mixing (Broadwell & Breidenthal 1982, Baker et al. 1984) in fog and derived an expression similar to Equation 3 but with a different supersaturation source term. The source of supersaturation, instead of vertical motion, is related to the rate at which interface between the mixed volumes is created, being proportional to $(1 - t/\tau_l)^{-3/2}$, where τ_l is the eddy turnover time for the largest scales in the flow. Gerber's modified supersaturation equation, coupled with a droplet growth model, predicts sudden rises in supersaturation due to the rapid increase of interfacial area during a mixing event, followed by a slow decay on the timescale of droplet growth. Interestingly, such ramp-cliff structures are a common manifestation of scalar intermittency in high-Reynolds-number flows (e.g., Warhaft 2000),

although supersaturation is not a conserved variable, so the analogy may not be accurate in the strictest sense. Finally, in Gerber's model, the resulting supersaturation fluctuations give rise to a significantly broader droplet size distribution and improve the comparison with droplet size measurements made in radiation fog.

Korolev & Isaac (2000) consider the process of isobaric mixing in entrainment zones in clouds, and show that for realistic gradients in temperature and vapor pressure at the tops of stratocumulus clouds supersaturations at least an order of magnitude higher than the typical (mean) supersaturations in clouds can be produced in isolated zones. This results in rapid condensation growth and potentially the formation of large droplets needed to initiate the collision-coalescence process.

Krueger et al. (1997) have developed a new approach to capturing the details of sub-grid scale mixing in cloud models by using Kerstein's (1991) linear eddy model, a one-dimensional representation of scalar fluctuations down to the dissipation scale. Details of sub-grid scale modeling (e.g., Cotton & Anthes 1989) are outside the scope of this review, but this particular model is mentioned because it has been extended by Su et al. (1998) to account for the growth of individual cloud droplets, so that droplet size distributions can be predicted. Essentially, the model is used to describe fluctuations in scalar quantities such as temperature and vapor density during a series of discrete entrainment events; then cloud-droplet growth in the local environment can be calculated.

Annu. Rev. Fluid Mech. 2003.35:183-227. Downloaded from www.annualreviews.org
by Fordham University on 01/19/13. For personal use only.

6. DROPLET GROWTH BY COLLISION AND COALESCENCE

Rain formation by collision-coalescence is a classic example of an aggregation process, but it also is notorious for the great uncertainty in the rate constants governing the process (e.g., Zangwill 2001). Turbulence likely plays a fundamental role in determining the rate constants (i.e., collision kernels) and perhaps even compounds the difficulties already inherent in measuring or calculating them. Here we discuss research suggesting that collision rates in clouds depend not only on droplet size, but also on properties of the turbulent flow in which the droplets reside.

6.1. Enhanced Droplet Settling and Relative Velocity

Dense particles in a turbulent flow can fall at speeds significantly different from the settling velocity in a quiescent fluid (e.g., Manton 1974, Maxey & Corrsin 1986, Maxey 1987, Wang & Maxey 1993). This has direct implications for the theory of collision and coalescence, for example, as pointed out by Pinsky & Khain (1996). In a recent study of particle motion near vortices, Dávila & Hunt (2001) have related fundamental droplet-settling regimes with two dimensionless parameters, a dimensionless terminal velocity V_T, and a particle Froude number F_p. These

Annu. Rev. Fluid Mech. 2003.35:183-227. Downloaded from www.annualreviews.org
by Fordham University on 01/19/13. For personal use only.

parameters are related to the dimensionless numbers defined in Section 4.1 in the form $V_T = S_d/F_f$ and $F_d = S_d^3/F_f^2$. For cloud droplets in a convective cloud, where the droplet terminal velocity (in still air) is less than the root mean-square fluid velocity, the actual fall speed of particles with finite inertia will be increased owing to interactions with the fluid turbulence (Dávila & Hunt 2001). Ghosh & Jonas (2001) have applied these results to an approximate equation for the growth of a large drop falling through a population of small cloud droplets, originally developed by Baker (1993). In the original model, the radius of a large drop r changes with time as $r(t) = r_0 \exp(t/\tau_c)$, where τ_c is a time constant inversely proportional to the liquid water content of the small droplets. When changes in the sedimentation speed of the large drop due to fluid accelerations are accounted for, a new time constant $\tau_c^* < \tau_c$ can be derived analytically, with the result that the model is in greater agreement with observations of large drop concentrations in stratocumulus clouds (Ghosh & Jonas 2001).

Khain & Pinsky (1995) considered the increase in volume swept out by a falling drop due to shear-induced velocity relative to the fluid. They modified the collision kernel with an rms relative velocity difference and showed that this could modify the rate at which rain is formed in clouds. Moving from simple shear flows to a full model of Batchelor turbulence, Pinsky & Khain (1997c) studied the relative motion of droplets with respect to the fluid, accounting for finite droplet inertia. In a companion paper, Khain & Pinsky (1997) studied the increase in swept volume in the simulated turbulence, as well as the resulting increase in the collision kernel, and its effects on the collision-coalescence process. The studies represent the first application of these concepts to flows with ranges of ϵ and droplet radius relevant to convective clouds. One potentially important limitation is the fact that the flow fields considered were all two-dimensional, as well as the fact that the turbulence model does not account for fine-scale intermittency.

With the aim of understanding the importance of acceleration intermittency on the collision kernel, Shaw & Oncley (2001) analyzed hot-wire velocity data from the atmospheric boundary layer as a surrogate for the high-Reynolds-number turbulence typically found in clouds. As expected, the energy dissipation ϵ was found to be extremely intermittent, and this was used to show that Lagrangian fluid accelerations in atmospheric turbulence can be up to $10g$. Such accelerations are expected to produce very large relative droplet velocities, with collision kernels enhanced by an order of magnitude at least, although only in isolated regions of the flow. Whether such intermittent spikes in the collision kernel will influence the rain formation process remains an open question.

6.2. Enhanced Collision Rates Due to Inertial Clustering of Droplets

Because the collision rate $\mathcal{N}_c \propto n^2$, it is a direct consequence of the density fluctuations discussed in Section 4.2 that $\mathcal{N}_c$ will be a fluctuating quantity as well. In essence, when droplet inertia is accounted for, the collision rate becomes a spatially

dependent function, being enhanced in regions of high strain and low vorticity. This is in addition to enhanced relative velocity and other turbulence effects described in the previous section. Pinsky & Khain (1997a,b) first introduced this notion to the cloud physics community and concluded that horizontal inhomogeneities would be most prominent at centimeter scales. Because the collision rate is nonlinear, the enhancement of $\mathcal{N}_c$ in regions of high droplet number density is greater than the reduction of $\mathcal{N}_c$ in droplet-depleted volumes. They accounted for this mechanism in the droplet-coagulation equation by adding a term proportional to the rms drop-velocity flux divergence.

Another method for including effects of number density fluctuations in the coagulation equation is given in the landmark paper by Sundaram & Collins (1997). They used the pair correlation function, or radial distribution function, to quantify the preferential concentration of monodisperse particles in isotropic turbulence. Specifically, they showed that the Saffman-Turner collision kernel (Saffman & Turner 1956) can be modified to account for spatial correlations by multiplying it by the radial distribution function evaluated at the particle diameter. The reason for this is approximately as follows. The number of collisions per unit time experienced by a single droplet in a population of identical droplets spatially distributed with perfect randomness is the product of the mean number density of droplets and the collision kernel, $\overline{n}\kappa$ (see Section 2). Given that there are $\overline{n}$ droplets per unit volume the total collision rate is $\mathcal{N}_c = \frac{1}{2}\overline{n}^2\kappa$. If, however, droplet positions are spatially correlated, then we must consider the conditional probability that a droplet will be found at a distance equal to the sum of the radii of the two droplets, the distance at which a collision is said to occur. As discussed in Section 3.2, the conditional probability of finding a droplet at a distance r from any given reference droplet is $P_{1,2}(\mathrm{r}) = \overline{n}dV(1 + \eta(\mathrm{r}))$, where $\eta(\mathrm{r})$ is the pair correlation function. Using the conditional probability per unit volume, the number of collisions per unit time experienced by a single droplet in a spatially correlated population of droplets of radius r is $\overline{n}(1 + \eta(r + r))\kappa$. Therefore, we can write a modified collision rate $\tilde{\mathcal{N}}_c = \frac{1}{2}\overline{n}^2(1 + \eta(2r))\kappa$. This result appears to be general for any statistically homogeneous population of droplets and any collision kernel. The collision rate between droplets of sizes r_1 and r_2 is $\tilde{\mathcal{N}}_c = \overline{n}_1\overline{n}_2(1 + \eta_{1,2}(r_1 + r_2))\kappa(r_1, r_2)$, where $\eta_{1,2}(\mathrm{r})$ is the pair correlation between droplets of size r_1 and r_2. The correct limit $\tilde{\mathcal{N}}_c = \mathcal{N}_c = \overline{n}_1\overline{n}_2\kappa(r_1, r_2)$ is obtained for a completely uncorrelated droplet spatial distribution where $\eta(\mathrm{r}) = 0$ at all scales.

Since the work by Sundaram & Collins (1997), there have been significant efforts given to quantifying the degree of enhancement of droplet collision rates when inertial effects are accounted for (e.g., Reade & Collins 2000, Wang et al. 2000). For the range of Stokes numbers considered in those studies, it was found that at scales below the Kolmogorov scale the radial distribution function has a power law form, increasing with decreasing scale until the finite size of the particle is reached (as might be expected from a small-r expansion of the autocorrelation function. Lending strength to this observation, the power law form of the pair correlation function has been obtained theoretically by Balkovsky et al. (2001). Also,

Annu. Rev. Fluid Mech. 2003.35:183-227. Downloaded from www.annualreviews.org
by Fordham University on 01/19/13. For personal use only.

Annu. Rev. Fluid Mech. 2003.35:183-227. Downloaded from www.annualreviews.org
by Fordham University on 01/19/13. For personal use only.

it has been pointed out that the range of Stokes numbers where significant inertial clustering occurs tends to become larger as the turbulence Reynolds number is increased over the modest ranges attainable in direct numerical simulations of turbulence (Reade & Collins 2000, Shaw et al. 1999). Shaw et al. (1999) argued that this may be a manifestation of the increasing intermittency at small scales, but additional work is needed to confirm or reject this hypothesis. Finally, Vaillancourt & Yau (2000) have pointed out that the majority of numerical and laboratory work has been focused on a range of parameter space (e.g., Stokes number, gravitational sedimentation) different from that occupied by atmospheric clouds. For example, the majority of direct numerical simulation studies have not accounted for gravity and have focused on Stokes numbers close to unity, where preferential concentration is observed to be most prominent (e.g., Hogan et al. 1999, Reade & Collins 2000, Sundaram & Collins 1997, Wang et al. 2000). Vaillancourt & Yau (2000) point out that, whereas for many engineering flows these are reasonable regions of parameter space to study, for the early processes in clouds the dissipation rates and droplet sizes are such that Stokes numbers are on the order of 10^{-2} and gravitational sedimentation is not negligible. The numerical simulation of droplet collision rates in turbulent flows approximating atmospheric conditions (noting, of course, that atmospheric Reynolds numbers will not be attainable) will be an important step in future work.

Very few experimental studies of droplet growth in turbulence, in parameter ranges of relevance to atmospheric clouds, have been reported in the literature; the study by Woods et al. (1972) is a notable exception. Recently, however, Vohl et al. (1999) have confirmed in a laboratory experiment that large drops suspended in a wind tunnel containing small droplets experience faster growth when the flow is turbulent than when it is laminar. They estimate that for drops starting at a radius of roughly 70 μm and growing to 180 μm, the collision kernel was increased by 10%–20% when turbulence was present, compared with the laminar, differential sedimentation velocity scenario. Clearly, there is a great need for further experimental studies of collision-coalescence in the presence of turbulence to complement theoretical and computational progress.

6.3. A Model of Collision-Coalescence in Mixing Zones

Here we extend the collision formulation described in Section 6.2 to the problem of entrainment and mixing in clouds. We consider a turbulent region of cloud where a mean gradient in n exists (e.g., at cloud top) so that fluctuations in n due to turbulent mixing lead to positive spatial correlations of droplet positions. It is assumed that fluctuations due to turbulent mixing cease at scales $r < \lambda_k$, so that the autocorrelation function of n is approximately 1 (its maximum value) over the same range of scales. The autocorrelation function of n can be predicted using a mixing theory or obtained directly from measurements in clouds. Then it is translated to the discrete language of the pair correlation function, with $\eta(r_{1,2})$ obtained via Equation 10 (note that $r_{1,2}$ is the scale at which two drops collide).

Assuming that $r_{1,2} < \lambda_k$, this results in $\eta(r_{1,2}) \approx \overline{n'^2}/\overline{n}^2$. We write the collision rate as $\tilde{\mathcal{N}}_c = \frac{1}{2}\overline{n}^2(1 + \eta(r_{1,2}))\kappa$ to account for spatial correlations, in this case due to turbulent mixing rather than inertial clustering of droplets. Therefore, for the mixing zone, $\tilde{\mathcal{N}}_c \approx (\overline{n}^2 + \overline{n'^2})\kappa = \overline{n^2}\kappa$. Because $\overline{n^2} \geq \overline{n}^2$, the actual collision rate in the mixing zone always is greater than the collision rate corresponding to perfect randomness, until complete mixing occurs so that no spatial correlations exist. We note that, although obtained by different reasoning, the $\overline{n^2}$ component of $\tilde{\mathcal{N}}_c$ is similar to the Reynolds stress terms in the collision equation considered by Stevens et al. (1998) in their critique of one- and two-dimensional cloud models.

The arguments in the preceding paragraph are general, and now we proceed to construct a conceptual model of collisions in the presence of nongradient mixing (Broadwell & Briedenthal 1982). This model is consistent with the common observation that the mixing process in clouds is characterized by sharp gradients and sudden jumps between two extreme states (such as number density), rather than smooth transitions (e.g., Baker et al. 1984, Brenguier 1993, Korolev & Mazin 1993, Malinowski et al. 1998, Paluch & Baumgardner 1989). We consider the turbulent mixing of two volumes containing cloud droplets initially distributed with perfect randomness, with number densities n_1 and n_2 and volume fractions ϕ_1 and ϕ_2 (where $\phi_1 + \phi_2 = 1$). Again, we assume that the minimum scale at which fluctuations are expected to exist is λ_k. Before this scale is reached, however, we make the assumption that the mixed region consists of "patches" of n_1 and n_2, with very sharp gradients separating them. These patches become finer and finer, the interfacial area growing with time, until the entire mixed volume is occupied by sharp gradients where molecular diffusion is efficient. In the theory of nongradient mixing, the surface area per unit volume grows as $(1/l)(1 - t/\tau_l)^{-3/2}$, which remains small until times close to τ_l, when it grows explosively. If the interfacial thickness where molecular diffusion is dominant is assumed to be δ, then the volume fraction of uniformly mixed fluid grows as $(\delta/l)(1 - t/\tau_l)^{-3/2}$, which for realistic cloud scales is negligibly small until reaching 1 at $t \approx \tau_l$. Now, until τ_l is reached, to good approximation the relative volume fractions ϕ_1 and ϕ_2 are preserved (although they are divided with increasing fineness). This allows us to write the collision rate as $\tilde{\mathcal{N}}_c \approx \overline{n^2}\kappa = (\phi_1 n_1^2 + \phi_2 n_2^2)\kappa$ until τ_l is reached and it relaxes to $\mathcal{N}_c \approx \overline{n}^2\kappa = (\phi_1 n_1 + \phi_2 n_2)^2\kappa$. Note that the first expression is the volume-weighted average of the collision rate for the two original volumes, and the second expression is the collision rate corresponding to the average number density after the two volumes are mixed thoroughly.

For the simple case of entrainment of dry air ($n_2 = 0$) the ratio of collision rates is $\tilde{N}_c/N_c = 1/\phi_1$, illustrating that the difference can become large depending on the volume fraction of entrained air. In a typical cloud model where mixing is assumed to take place instantaneously on sub-grid scales it is clear that the collision rate is consistently underpredicted and that improvements are needed if small-scale variability is to be accounted for properly.

Annu. Rev. Fluid Mech. 2003.35:183-227. Downloaded from www.annualreviews.org
by Fordham University on 01/19/13. For personal use only.

Annu. Rev. Fluid Mech. 2003.35:183-227. Downloaded from www.annualreviews.org
by Fordham University on 01/19/13. For personal use only.

6.4. Collision Efficiency

As pointed out in Section 2, the collision efficiency accounts for departures from the behavior of a hard-sphere model, where interdroplet interactions are not present. These departures are very significant for cloud droplets in air, with efficiencies smaller than 0.01 being possible (e.g., Pruppacher & Klett 1997). Physically, the combined effect of collision and coalescence efficiencies are due to the microhydrodynamics of interacting droplets, Van der Waals forces, etc., and the details cannot be treated here because of space limitations. However, several recent advances in accounting for effects of turbulence in the collision efficiency are mentioned. Pinsky et al. (1999b, 2000) point out that, because the collision efficiency is sensitive to droplet relative velocity, in a cloud the efficiency must account not only for differential sedimentation, but also for relative velocities due to flow accelerations. The model by Pinsky and coworkers of droplet motion in turbulent flow results in inertia-induced relative velocities that can exceed the gravitationally induced relative velocities for droplets with radii less than 30 μm. In this size range, they are able to use the Stokes-flow-superposition approach to obtain collision efficiencies for various flow-induced configurations (droplet relative velocity and approach angle). As a result, they conclude that the collision efficiency must be considered a random variable, and that its magnitude typically is larger than the gravitational efficiency by several times for the droplet size range considered. In a later study, Pinsky et al. (2001) extended this type of analysis to higher droplet Reynolds numbers to obtain collision efficiencies for droplets with radii up to 300 μm. In addition, they demonstrated a significant pressure dependence on the collision efficiency that is relevant to cloud processes because of the large pressure changes that occur during cloud growth.

7. MEASUREMENTS IN TURBULENT CLOUDS

Measurements of cloud properties are challenging because clouds are transient and usually must be studied remotely, often requiring complex data inversions, or with airborne instrument platforms, which are expensive and come with severe constraints on instrument size and data rate. (Obvious exceptions are low clouds and fog, which can be studied in situ from towers or mountaintop observatories, for example.) In spite of the inherent challenges, such measurements are of great value in quantifying complex interactions over large ranges of spatial and temporal scales characteristic of geophysical systems. And, of course, measurements from real clouds are of crucial importance for guiding theoretical, computational, and laboratory work.

In addition to physical challenges inherent in making measurements in clouds, there are challenges associated with making measurements of a strongly fluctuating, random system. For example, how deterministic models of cloud processes such as condensation growth should be compared with actual observations is an

open question (e.g., Oreskes et al. 1994). In one approach, Liu et al. (1995) and Liu & Hallett (1998) have argued via Shannon's maximum entropy principle and energy considerations, that it is possible to derive most-probable and least-probable functional forms for a droplet size distribution. Under the constraints of conserved mass and number, the most probable size distribution is a Weibull function and the least probable is a delta function. Any finite measurement, therefore, will result in a distribution between the two limits, so it becomes necessary to consider the probabilistic nature of the problem when comparing measurements and theory. This must be coupled with the aforementioned caution that clouds and instrument sampling volumes are finite, so the size distribution $f(r)$ can only be estimated. As with any random system, statistical measures such as means and variances are meaningful only if the system is statistically homogeneous or stationary (e.g., Jameson & Kostinski 2000, 2001).

In this section, we highlight some of the most recent advances that are revealing, for the first time, the fine-scale structure of turbulent clouds. We begin by discussing measurements of continuous variables, such as velocity and temperature, and we end with a review of recent efforts to quantify the spatial distribution of cloud droplets in turbulent clouds.

Annu. Rev. Fluid Mech. 2003.35:183-227. Downloaded from www.annualreviews.org
by Fordham University on 01/19/13. For personal use only.

7.1. Turbulence

Interactions between turbulence and cloud microphysics occur on very small scales. Unfortunately, however, the spatial resolution of most aircraft-based measurements typically are limited to m scales and above because of the high speeds of research aircraft. Compounding this, there are problems associated with flow distortions and compressibility effects in airborne measurements of scalar quantities in turbulence (Wyngaard 1988). Furthermore, some traditional techniques for measuring fine-scale turbulence in the atmospheric boundary layer are hindered by the presence of water droplets in clouds (e.g., hot-wire anemometry). Here we briefly discuss several new approaches to making high-resolution measurements of temperature and velocity fluctuations in turbulent clouds.

Recent advances in instrument design have made rapid measurements of temperature possible in clouds, allowing centimeter scales to be resolved (Haman et al. 1997, 2001). Temperature measurements at small scales (high sampling rates) have been limited in the past by difficulties associated with the presence of water droplets and their tendency to wet fine, hot-wire probes. These measurements have provided a new picture of fine-scale temperature fluctuations inside clouds. For example, all clouds investigated are characterized by sudden jumps between different temperatures, with the scales between jumps varying from tens of meters to several centimeters. The sharp temperature gradients where diffusion is active are possible sites for the formation of large supersaturations due to isobaric mixing (Gerber 1991, Korolev & Isaac 2000). In addition, the measurements have revealed that the power spectrum of temperature fluctuations exhibits a shallower slope than $-5/3$ on spatial scales smaller than $\sim$1 m. This is analogous to the enhanced variance observed in power spectra of liquid water content on sub-m scales

(Davis et al. 1999, Gerber et al. 2001). For temperature, the enhanced variance could be due, in part, to fluctuations in droplet growth rate in mixing zones and the resultant heating due to the enthalpy of vaporization of water. On the other hand, the shallower slope in temperature and liquid water content power spectra may be a more general property of passive scalars or small inert particles suspended in turbulent fluid, such as the viscous-convective subrange (Batchelor 1959; Jeffery 2000, 2001a; Warhaft 2000).

Methods for making velocity measurements on sub-m scales, such as using balloon-borne sonic anemometers in clouds (Siebert & Teichmann 2000), are under development. Also, it will be some time before fine-scale Lagrangian accelerations in turbulent clouds can be measured directly. However, a method for quantifying Lagrangian accelerations in clouds has been suggested by Hill (2002). As discussed in Section 3, Hill has shown that in the large Reynolds number limit $\langle a_L^2 \rangle \propto \overline{\epsilon}^{3/2} \nu^{-1/2} \mathrm{R}_\lambda^{1/4}$. Hill has pointed out that both ϵ and u_{rms} can be measured using radar, making a calculation of $\mathrm{R}_\lambda = u_{rms}^2/(\epsilon\nu/15)$ and the variance of Lagrangian acceleration possible.

Annu. Rev. Fluid Mech. 2003.35:183-227. Downloaded from www.annualreviews.org
by Fordham University on 01/19/13. For personal use only.

7.2. Measurements of Spatially Dependent Clustering

Throughout this review we have returned repeatedly to the question of how droplets are distributed in space. It is a fundamental element of theories of condensation growth (e.g., Srivastava 1989), collision and coalescence (e.g., Pinsky & Khain 1997a), and radiative transfer in clouds (e.g., Kostinski 2001, Marshak et al. 1998, Shaw et al. 2002a), and therefore is of great relevance. Until recently, however, the question does not appear to have been addressed from an experimental perspective, except in the pioneering work of Kozikowska et al. (1984). During the past decade, there has been an explosion of experimental work on the fine-scale (less than 1 m) properties of clouds (e.g., Baker 1992, Baumgardner et al. 1993, Borrman et al. 1993, Brenguier 1993, Chaumat & Brenguier 2001, Davis et al. 1999, Gerber et al. 2001, Kostinski & Shaw 2001, Pinsky & Khain 2001, Uhlig et al. 1998). Much of this progress has been made possible by the advent of high-data-rate probes (e.g., Baumgardner et al. 1993, Brenguier et al. 1998, Gerber et al. 1994), which have opened a new window on the small-scale features of clouds.

Several new instruments that allow cloud-droplet measurements with cm-scale resolution or better are the cloud particle imager (CPI) (Lawson & Cormack 1995), which takes snapshots of small (2 to 50 mm^3) volumes of cloud; the particle volume monitor (PVM) (e.g., Gerber et al. 1994), which makes high-spatial-resolution (cm-scale) liquid water content measurements; and the Fast FSSP (Brenguier et al. 1998), an improved version of a standard instrument, the FSSP-100. With the Fast FSSP, pulse duration and interarrival times (due to droplets moving past a laser beam) are measured with a 16 MHz clock or a distance of approximately 6 μm along the aircraft track. The area of the depth of field, where droplet size can be measured, is 0.13 mm^2, whereas the total sampling area is 3 mm^2. Thus, the total sampling volume for the Fast FSSP can be considered a long, narrow tube (Chaumat & Brenguier 2001).

Once an instrument sampling volume has been defined, it becomes necessary to develop tools for quantifying the degree of randomness in the droplet spatial distribution. One possible approach is to divide the volume—for example, the long narrow tube from the Fast FSSP—into equally sized volume elements V. Then the number of droplets counted in each volume element N becomes a countable, random number. It is a property of the Poisson distribution that the variance in droplet counts is equal to the mean number of droplet counts. Therefore it is natural to define the clustering index (CI) as the variance-to-mean ratio,

$$CI(V) = \frac{\overline{(\delta N)^2}}{N} - 1, \tag{20}$$

where N is the random number of droplets in a volume, $\bar{N}$ is the mean number of droplets, and $\overline{(\delta N)^2} \equiv \overline{(N - \bar{N})^2}$ is the variance. The CI (also fishing test) was first applied to the analysis of cloud-droplet spacing by Baker (1992). The CI is zero for the Poisson distribution (for any given test volume V) and becomes positive when positive spatial correlations are dominant in V. It has been used by several groups to quantify the degree of droplet clustering in clouds (Baker 1992, Chaumat & Brenguier 2001, Uhlig et al. 1998, Vaillancourt et al. 2002), with various results. Baker (1992) analyzed high-frequency measurements from a particle detection probe (FSSP) and showed that in mixing regions the CI can become very large, illustrating the strong correlations between droplet positions. He argued that for some data series the clustering was anomalously large at small scales, suggesting that some mechanism was operating to cause enhanced droplet clustering.

An especially attractive approach for investigating the spatial distribution of cloud droplets is in-line holography (e.g., Borrmann & Jaenicke 1993, Kozikowska et al. 1984). The technique also can be extended to three-dimensional velocimetry, as has been done in laboratory flows (e.g., Pu & Meng 2000). Borrmann et al. (1993) and Uhlig et al. (1998) used a holographic imaging system to study the three-dimensional distribution of cloud droplets in low stratus. In the earlier paper, they reported, based on a single hologram, no deviation from perfect randomness. Based on an analysis of the CI and interdroplet frequency distributions, however, Uhlig et al. (1998) concluded that there were significant departures from uniform probability of particle positions. In both cases the turbulence was not quantified, and it is not clear to what extent entrainment and mixing contributed to this departure from pure randomness. In all of the holography studies, the amount of data obtained was limited by the time-consuming data processing, which involves reconstruction of the hologram and subsequent measurements of particle position. In spite of this, a significant advantage of the holography approach is the ability to measure directly the three-dimensional distribution of droplets, thereby avoiding difficulties associated with the projection into two or one dimension (Holtzer & Collins 2002).

Chaumat & Brenguier (2001) have conducted the most thorough study to date of droplet clustering in turbulent clouds, having analyzed data from many traverses through cumulus clouds during the Small Cumulus Microphysics Study (SCMS).

Annu. Rev. Fluid Mech. 2003.35:183-227. Downloaded from www.annualreviews.org
by Fordham University on 01/19/13. For personal use only.

Annu. Rev. Fluid Mech. 2003.35:183-227. Downloaded from www.annualreviews.org
by Fordham University on 01/19/13. For personal use only.

The data were obtained using the Meteo-France Fast FSSP, described previously, and an example of a single traverse is shown in Figure 2. A primary goal was to determine the degree of droplet clustering that occurs on small scales as a result of factors such as particle inertia. Therefore, they were careful to confine their analysis to undiluted cloud cores to minimize the effects of mixing on the cloud-droplet spatial distributions. Their general conclusion was that the degree of clustering on cm scales and below is within the limits of uncertainty of the *CI*. Furthermore, they argued that even if the the small degree of clustering observed was real it would be insufficient to cause any significant change in the width of the droplet size distribution.

In a study using a single traverse during SCMS, Kostinski & Shaw (2001) searched for scale-dependent clustering of droplets in a core region of the cloud where mixing was expected to be negligible. They argued that a scale-localized measure of clustering must be used to do this unambiguously. For example, they argued that clustering on a given scale can be masked by "scale-memory" of instrument resolution when the *CI* is used. This is because the *CI* represents contributions from a range of scales (including all scales below the instruments' resolution limit) and therefore possesses an inherent volume dependence. Indeed, the explicit link between *CI* and the scale-localized pair correlation function is given by the correlation-fluctuation theorem (e.g., Landau & Lifshitz 1980, Section 116; Kostinski & Jameson 2000; Shaw et al. 2002b)

$$\frac{\overline{(\delta N)^2}}{N} - 1 = \bar{n} \int_0^V \eta(V')\, dV'. \tag{21}$$

Hence, the *CI* is said to contain memory of all scales within volume *V*. However, Equation 21 gives a clear approach for obtaining a scale-localizable measure of droplet clustering from *CI*. Using the pair correlation function, Kostinski & Shaw (2001) concluded that statistically significant clustering was present at centimeter scales and below, thereby providing evidence for fine-scale droplet-turbulence interactions in the atmosphere. The scales identified as having positive correlations correspond to those expected for finite droplet inertia. In the study by Kostinski & Shaw (2001), no conclusions were drawn on whether the magnitude of the clustering was sufficiently large to affect cloud processes such as condensation growth or collision-coalescence. As a final note, we remark that Holtzer & Collins (2002) have recently demonstrated that when a three-dimensional field of droplets is sampled in two or one dimension (as with the Fast FSSP), the pair correlation function is strongly suppressed at scales less than the averaging scale of the instrument. For pair correlation functions following a power law dependence with r (e.g., Balkovsky et al. 2001, Reade & Collins 2000), they provided an inversion technique for estimating the full three-dimensional function needed for the collision rate modifications discussed in Section 6.

An example of the one-dimensional pair correlation function for cloud droplets is shown in Figure 8. It corresponds to the entire traverse shown in Figure 2 and

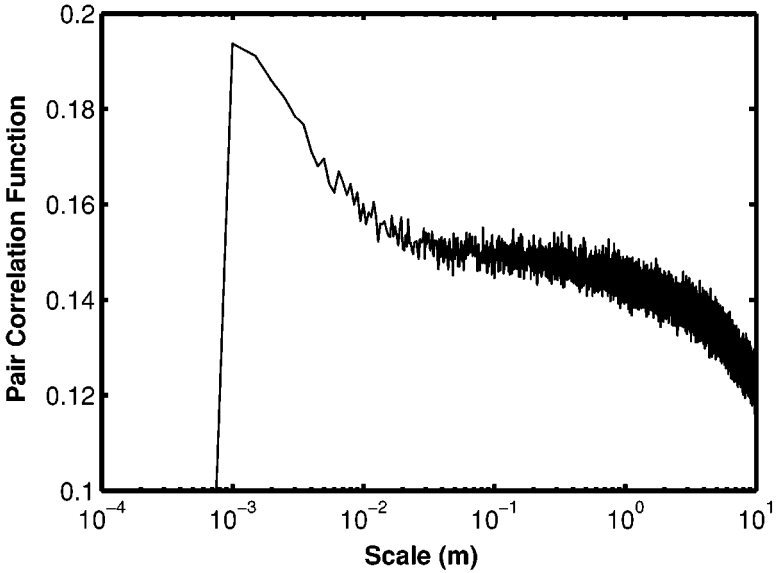

Figure 8 The one-dimensional pair correlation function for the cumulus cloud traverse shown in Figure 2. At large scales, the pair correlation function decays to zero, as does the autocorrelation function. The enhanced clustering on millimeter and centimeter scales is consistent with the inertial clustering hypothesis. Scales below 1 mm are lost as a result of the finite resolution of the instrument. Adapted from Shaw et al. (2002b), data courtesy of J.-L. Brenguier, Meteo-France.

Annu. Rev. Fluid Mech. 2003.35:183-227. Downloaded from www.annualreviews.org
by Fordham University on 01/19/13. For personal use only.

therefore accounts for spatial correlations up to scales of 100 m (above which the pair correlation function goes to zero, as expected) as well as strong correlations on centimeter scales and below. The enhanced clustering on millimeter and centimeter scales is consistent with the inertial clustering hypothesis, which would suggest that the clustering continues to increase at scales below 1 mm. This is not detected because of the finite resolution of the instrument.

Using a different approach to analyze Fast FSSP data from SCMS, Pinsky & Khain (2001) also concluded that there was significant droplet clustering on centimeter scales and below. They took the viewpoint of an inhomogeneous Poisson process, with the large-scale fluctuations in the mean droplet number density modeled by a Fourier series with coefficients weighted for best fit. The remaining small-scale fluctuations were found to be in excess of those expected, with the root mean-square fluctuation equal to approximately 30% of the mean number density. Fluctuations between 0.5 and 5 cm were found to be dominant, thus providing evidence for the droplet inertial clustering mechanism.

Fine-scale measurements of liquid water content, which is proportional to $\int_0^\infty f(r)r^3dr$, have been obtained with the PVM instrument (Gerber et al. 1994).

Annu. Rev. Fluid Mech. 2003.35:183-227. Downloaded from www.annualreviews.org
by Fordham University on 01/19/13. For personal use only.

These observations have revealed strongly enhanced variability of liquid water content (Davis et al. 1999, Gerber et al. 2001, Marshak et al. 1998) in turbulent clouds. By enhanced, it is meant that the slope of the scalar-variance power spectrum is much shallower than $-5/3$ at frequencies corresponding to spatial scales of less than a few meters. A power spectrum of liquid water content is shown in Figure 7. The one-dimensional scalar spectrum for liquid water content data obtained during the SOCEX field experiment is shown as open squares (Marshak et al. 1998). The observed spectrum is an order of magnitude larger than the typical inertial-convective and viscous-convective scaling, which is shown by the solid line (Jeffery 2001b). This variance has been attributed to several causes, including enhanced entrainment of dry air at small scales (Gerber et al. 2001) and droplet clustering (Davis et al. 1999), but no details were given regarding the physical mechanisms for such processes. Mazin (1999) has pointed out that the observed enhancement in variability at small scales occurs as turbulence frequencies become greater than the inverse of the phase relaxation time and therefore is in agreement with the theory of stochastic condensation.

In Section 4.2 Jeffery's (2000, 2001b) spectral scaling for liquid water content fluctuations due to finite droplet inertia was discussed. Associated with the increased scalar dissipation rate, the theory suggests that the inertial-convective subrange is extended to smaller scales, with transition to the viscous-convective subrange occurring at scales of approximately $60\lambda_k$ or several centimeters. This, however, is in contrast to observations of liquid water content fluctuations in turbulent clouds, where the transition to a regime with enhanced variance is observed to take place at scales of approximately 2–5 m (see Figure 7). An explanation for these observations has been proposed by Jeffery (2001a,b), who argues that the new regime shown in Figure 7 is a manifestation of number density fluctuations due to both finite droplet inertia and the condensation process. In effect, particle inertia leads to an enhanced viscous-convective subrange, but which begins at frequencies higher than observed. When the condensation process is accounted for, however, a production range lying between the inertial subrange and the viscous-convective subrange exists. This tends to enhance scalar variance at larger scales (up to tens of centimeters, an order of magnitude larger than for inertial effects alone), thereby providing a plausible theory for explaining observations of liquid water content fluctuations. The evaporation/condensation model of Jeffery (2001a) predicts a fundamental inhomogeneity in vertical fluctuations of liquid water content, with their magnitude increasing with height above cloud base. As pointed out by Jeffery, this is in qualitative agreement with many observational and computational studies of turbulent clouds.

An additional technique for determining the spatial distribution of particles in clouds is analogous to in X-ray scattering from liquids, where Bragg scattering measurements yield the Fourier transform of the pair correlation function. By investigating Bragg scattering of coherent radiation emitted by radars, it is possible, in principle, to detect droplet clustering that occurs on spatial scales of similar magnitude as the radar wavelength (Kostinski & Jameson 2000). Recently,

several investigators have noted anomalous Bragg returns in radar measurements of small cumulus clouds (Baker & Brenguier 1998, Knight & Miller 1998) and smoke plumes (Rogers & Brown 1997). Indeed, Jameson & Kostinski (2000) point out that the radar measurements by Knight & Miller (1998), which show a correlation between Rayleigh and Bragg returns in some cases, support the idea that scale-dependent correlations in particle positions may be responsible for the Bragg signal. Baker & Brenguier (1998) suggest that enhanced Bragg signals that existed even when strong mixing was not present may be caused by clustering of droplets due to their finite inertia. In a recent contribution, Erkelens et al. (2001) also argue that fluctuations in liquid water content can produce coherent (Bragg) scattering that exceeds the incoherent component typically considered. They compared a model of liquid water content fluctuations due to mixing to radar returns from cumulus clouds and smoke and found evidence for the existence of Bragg scattering. Significant Bragg scattering also occurred in cloud regions where no mixing had taken place and they suggest that this is evidence for spatial clustering due to the finite inertia of cloud droplets.

Annu. Rev. Fluid Mech. 2003.35:183-227. Downloaded from www.annualreviews.org
by Fordham University on 01/19/13. For personal use only.

8. FINAL REMARKS

We summarize by reviewing several of the fundamental dimensionless numbers that are expected to be of relevance to the fluid mechanics of small-scale processes in atmospheric clouds: turbulence Reynolds number R_t, droplet Stokes number S_d, and turbulence acceleration ratio F_f. Obviously other quantities such as Richardson number are relevant in certain cases, but they have not been focused on here. The parameter space (in terms of the three variables mentioned) occupied by the archetype convective cloud is quite large. For a typical convective cloud, such as a cumulus with moderate energy dissipation rates and realistic droplet sizes, we can estimate $S_d \sim 10^{-3}$–10^{-1}, $F_f \sim 10^{-1}$–10^{1}, $R_t \sim 10^{6}$–10^{8}.

An additional dimensionless number of relevance to the thermodynamics of turbulent atmospheric clouds is the supersaturation Damköhler number $D_s = \tau_f/\tau_s$. This, essentially, determines the spatial and temporal scales at which supersaturation in a turbulent flow can be considered well mixed. For typical cumulus clouds the spatial scale at which $D_s \sim 1$ is on the order of several meters. This implies, therefore, that cloud droplet growth is influenced by turbulent fluctuations occuring in both large and small Damköhler number limits.

Although much work remains, at least in principle the parameter range for Stokes number can be attained in numerical and laboratory studies of turbulent flows containing appropriately sized particles. It is the Reynolds number similarity and the resulting intermittency in the acceleration ratio that places atmospheric clouds in a truly unique regime within the parameter space, separate from many multiphase flows existing in laboratories or industrial processes. For example, simulated turbulence and laboratory turbulence typically are limited to lower Reynolds numbers and much higher energy dissipation rates (with some exceptions). Therefore, we have considered how droplet-fluid interactions might change

with Reynolds number. Several issues relating to the Reynolds number scaling come to mind:

1. We know that intermittency of ϵ and Lagrangian fluid accelerations increases with Reynolds number (e.g., Hill 2002, Sreenivasan & Antonia 1997), but what aspects of the droplet growth are affected by this?
2. Physical properties of coherent vortex structures at small scales are thought to be strongly dependent on Reynolds number. How do these properties change and how does this affect cloud processes?
3. The nature of passive scalars advected by turbulent flows is known to be strongly linked to the Reynolds number (e.g., Warhaft 2000). How will this scalar intermittency manifest itself in turbulent clouds? For example, ramp-cliff structures in the thermodynamic fields such as temperature or supersaturation likely are related to Reynolds number.

Annu. Rev. Fluid Mech. 2003.35:183-227. Downloaded from www.annualreviews.org
by Fordham University on 01/19/13. For personal use only.

We emphasize here one of the special features of multiphase flows in general and clouds in particular: Essential processes that govern the evolution of the entire system take place at the scale of the particle size, which is smaller than the dissipation scale. Thus, the physical nature of turbulence at the smallest scales potentially is of vital importance to the cloud problem. Furthermore, it is well established that the small scales in turbulent flows are strongly dependent on the turbulence Reynolds number, so we expect that this will be an important parameter to consider. This is not to say that the large-scale structure of the cloud is not of equal importance: For example, fundamental work remains to be done on the role of entrainment of dry, noncloudy air on the evolution of clouds and the droplet distributions therein. Another aspect of the problem is the macroscopic variation of relevant dimensionless parameters throughout the cloud. For example, it is known that cloud boundaries typically contain the highest energy dissipation rates, whereas cloud cores may only contain weak turbulence.

We have reviewed the essential physics of fine-scale turbulence and its effects on clouds and have focused on two routes by which turbulence interacts with the evolution of droplet size distributions in atmospheric clouds. First, turbulence influences droplet growth via the thermodynamic process of condensation in a supersaturated environment. Second, turbulence influences droplet growth via the dynamical interaction of droplets in the collision-coalescence process. Understanding the nature of these processes, and separating the two in actual measurements, is a significant challenge that remains before us. No doubt the simultaneous use of theoretical, computational, laboratory, and fieldwork tools will be necessary to make continued progress.

ACKNOWLEDGMENTS

This review was initiated, in part, as a result of a workshop on the same topic sponsored by the Geophysical Turbulence Program of the National Center for Atmospheric Research in Boulder, Colorado. The interaction with colleagues

there, as well as the support of NCAR/GTP (see http://www.asp.ucar.edu/gtp/cloud2000.html for details of workshop, including a list of participants) is gratefully acknowledged. I also acknowledge the research support of the National Science Foundation, Atmospheric Sciences Division, Physical Meteorology Program. I thank W. Cantrell, G. Feingold, C. Jeffery, A. Kostinski, M. Larsen, and M. Wertheim for stimulating discussions and helpful comments. Finally, special thanks go to K. Sreenivasan and J. Wyngaard for their encouragement on this article.

The *Annual Review of Fluid Mechanics* is online at http://fluid.annualreviews.org

Annu. Rev. Fluid Mech. 2003.35:183-227. Downloaded from www.annualreviews.org
by Fordham University on 01/19/13. For personal use only.

LITERATURE CITED

Austin PH, Baker MB, Blyth AM, Jensen JB. 1985. Small-scale variability in warm continental cumulus clouds. *J. Atmos. Sci.* 42:1123–38

Baker BA. 1992. Turbulent entrainment and mixing in clouds: a new observational approach. *J. Atmos. Sci.* 49:387–404

Baker BA, Brenguier J-L. 1998. Unknown source of reflectivity from small cumulus clouds. *Conf. Cloud Phys.*, pp. 148–51. Everett, WA: Am. Meterol. Soc.

Baker MB. 1993. Variability in concentrations of cloud condensation nuclei in the marine cloud-topped boundary layer. *Tellus* 45B:458–72

Baker MB, Breidenthal RE, Choularton TW, Latham J. 1984. The effects of turbulent mixing in clouds. *J. Atmos. Sci.* 41:299–304

Balkovsky E, Falkovich G, Fouxon A. 2001. Intermittent distribution of inertial particles in turbulent flows. *Phys. Rev. Lett.* 86:2790–93

Batchelor GK. 1959. Small-scale variation of convected quantities like temperature in turbulent fluid. Part I: general discussion and the case of small conductivity. *J. Fluid Mech.* 5:113–33

Baumgardner D, Baker B, Weaver K. 1993. A technique for the measurement of cloud structure on centimeter scales. *J. Atmos. Ocean. Technol.* 10:557–65

Bayewitz MH, Yerushalmi J, Katz S, Shinnar R. 1974. The extent of correlations in a stochastic coalescence process. *J. Atmos. Sci.* 31:1604–14

Beard KV, Ochs HT. 1993. Warm-rain initiation: an overview of microphysical mechanisms. *J. Appl. Meteorol.* 32:608–25

Belin F, Maurer J, Tabelin P, Williame H. 1997. Velocity gradient distributions in fully developed turbulence: an experimental study. *Phys. Fluids* 9:3843–50

Berry EX, Reinhardt RL. 1974. An analysis of cloud drop growth by collection: part II. Single initial distributions. *J. Atmos. Sci.* 31:1825–31

Blyth A. 1993. Entrainment in cumulus clouds. *J. Appl. Meteorol.* 32:626–41

Borrmann S, Jaenicke R. 1993. Application of microholography for ground-based in situ measurements in stratus cloud layers: a case study. *J. Atmos. Ocean. Technol.* 10:277–93

Borrmann S, Jaenicke R, Neumann P. 1993. On spatial distributions and inter-droplet distances measured in stratus clouds with in-line holography. *Atmos. Res.* 29:229–45

Brenguier J-L. 1990. Parameterization of the condensation process in small nonprecipitating cumuli. *J. Atmos. Sci.* 47:1127–48

Brenguier J-L. 1993. Observations of cloud microstructure at the centimeter scale. *J. Appl. Meteorol.* 32:783–93

Brenguier J-L, Bourrianne T, Coelho AA, Isbert J, Peytavi R, et al. 1998. Improvements of droplet size distribution measurements with the Fast-FSSP (Forward Scattering Spectrometer Probe). *J. Atmos. Ocean. Technol.* 15:1077–90

Brenguier J-L, Chaumat L. 2001. Droplet spectra broadening in cumulus clouds.

Annu. Rev. Fluid Mech. 2003.35:183-227. Downloaded from www.annualreviews.org
by Fordham University on 01/19/13. For personal use only.

Part I: broadening in adiabatic cores. *J. Atmos. Sci.* 58:628–41

Broadwell JE, Breidenthal RE. 1982. A simple model of mixing and chemical reaction in a turbulent shear layer. *J. Fluid Mech.* 125:397–410

Cadot O, Douady S, Couder Y. 1995. Characterization of the low-pressure filaments in a three-dimensional turbulent shear flow. *Phys. Fluids* 7:630–46

Chaumat L, Brenguier JL. 2001. Droplet spectra broadening in cumulus clouds. Part II: microscale droplet concentration heterogeneities. *J. Atmos. Sci.* 58:642–54

Cooper WA. 1989. Effects of variable droplet growth histories on droplet size distributions. Part I: theory. *J. Atmos. Sci.* 46:1301–11

Corrsin S, Lumley J. 1956. On the equation of motion for a particle in turbulent fluid. *Appl. Sci. Res.* 6A:114–16

Cotton WR, Anthes RA. 1989. *Storm and Cloud Dynamics.* San Diego, CA: Academic

Dávila J, Hunt JCR. 2001. Settling of small particles near vortices and in turbulence. *J. Fluid Mech.* 440:117–45

Davis AB, Marshak A, Gerber H, Wiscombe WJ. 1999. Horizontal structure of marine boundary layer clouds from centimeter to kilometer scales. *J. Geophys. Res.* 104:6123–44

Dernoncourt B, Pinton J-F, Fauve S. 1998. Experimental study of vorticity filaments in a turbulent swirling flow. *Phys. D* 117:181–90

Eaton JK, Fessler JR. 1994. Preferential concentration of particles by turbulence. *Int. J. Multiph. Flow* 20:169–208

Elperin T, Kleeorin N, Rogachevskii I. 1996. Self-excitation of fluctuations of inertial particle concentration in turbulent fluid flow. *Phys. Rev. Lett.* 77:5373–76

Elperin T, Kleeorin N, Rogachevskii I. 1998. Anomalous scalings for fluctuations of inertial particles concentration and large-scale dynamics. *Phys. Rev. E* 58:3113–24

Elperin T, Kleeorin N, Rogachevskii I. 2000. Mechanisms of formation of aerosol and gaseous inhomogeneities in the turbulent atmosphere. *Atmos. Res.* 53:117–29

Erkelens JS, Venema VKC, Russchenberg HWJ, Ligthart LP. 2001. Coherent scattering of microwaves by particles: evidence from clouds and smoke. *J. Atmos. Sci.* 58:1091–102

Feingold G, Chuang PY. 2002. Analysis of the influence of film-forming compounds on droplet growth: implications for cloud microphysical processes and climate. *J. Atmos. Sci.* 59:2006–18

Fuchs NA. 1989. *The Mechanics of Aerosols.* New York: Dover

Gerber H. 1991. Supersaturation and droplet spectral evolution in fog. *J. Atmos. Sci.* 48:2569–88

Gerber H, Arends G, Ackerman AK. 1994. New microphysics sensor for aircraft use. *Atmos. Res.* 31:235–52

Gerber H, Jensen JB, Davis AB, Marshak A, Wiscombe WJ. 2001. Spectral density of cloud liquid water content at high frequencies. *J. Atmos. Sci.* 58:497–503

Ghosh S, Jonas PR. 2001. Some analytical calculations on the effect of turbulence on the settling and growth of cloud droplets. *Geophys. Res. Lett.* 28:3883–86

Grabowski WW. 1993. Cumulus entrainment, fine-scale mixing, and buoyancy reversal. *Q. J. R. Meteorol. Soc.* 119:935–56

Grabowski WW, Vaillancourt P. 1999. Comments on "Preferential concentration of cloud droplets by turbulence: effects on the early evolution of cumulus cloud droplet spectra." *J. Atmos. Sci.* 56:1433–36

Haman KE, Makulski A, Malinowski SP, Busen R. 1997. A new ultrafast thermometer for airborne measurements in clouds. *J. Atmos. Ocean. Technol.* 14:217–27

Haman KE, Malinowski SP, Struś BD, Busen R, Stefko A. 2001. Two new types of ultrafast aircraft thermometer. *J. Atmos. Ocean. Technol.* 18:117–34

Hill RJ. 2002. Scaling of acceleration in locally isotropic turbulence. *J. Fluid Mech.* 452:361–70

Hill RJ, Thoroddsen ST. 1997. Experimental

Annu. Rev. Fluid Mech. 2003.35:183-227. Downloaded from www.annualreviews.org
by Fordham University on 01/19/13. For personal use only.

evaluation of acceleration correlations for locally isotropic turbulence. *Phys. Rev. E* 55:1600–6

Hill RJ, Wilczak JM. 1995. Pressure structure functions and spectra for locally isotropic turbulence. *J. Fluid Mech.* 296:247–69

Hill TA, Choularton TW. 1985. An airborne study of the microphysical structure of cumulus clouds. *Q. J. R. Meteorol. Soc.* 111:517–44

Hogan RC, Cuzzi JN, Dobrovolskis AR. 1999. Scaling properties of particle density fields formed in simulated turbulent flows. *Phys. Rev. E* 60:1674–80

Holtzer GL, Collins LR. 2002. Relationship between the intrinsic radial distribution function for an isotropic field of particles and lower-dimensional measurements. *J. Fluid Mech.* 459:93–102

IPCC (Intergovernmental Panel on Climate Change) Working Group I. 1996. *Climate Change 1995: The Science of Climate Change*, ed. JT Houghton, LG Meira Filho, BA Callander, N Harris, A Kattenberg, K Maskell. Cambridge, UK: Cambridge Univ. Press

Jameson AR, Kostinski AB. 2000. Fluctuation properties of precipitation. Part VI: observations of hyperfine clustering and drop size distribution structures in three-dimensional rain. *J. Atmos. Sci.* 57:373–88

Jameson AR, Kostinski AB. 2001. Reconsideration of the physical and empirical origins of Z-R relations in radar meteorology. *Q. J. R. Meteorol. Soc.* 127:517–38

Jeffery CA. 2000. Effect of particle inertia on the viscous-convective subrange. *Phys. Rev. E* 61:6578–85

Jeffery CA. 2001a. Effect of condensation and evaporation on the viscous-convective subrange. *Phys. Fluids* 13:713–22

Jeffery CA. 2001b. Investigating the small-scale structure of clouds using the δ-correlated closure: effect of particle inertia, condensation/evaporation and intermittency. *Atmos. Res.* 59/60:199–215

Jensen JB, Baker MB. 1989. A simple model of droplet spectral evolution during turbulent mixing. *J. Atmos. Sci.* 46:2812–29

Jiménez J, Wray AA, Saffman PG, Rogallo RS. 1993. The structure of intense vorticity in isotropic turbulence. *J. Fluid Mech.* 255:65–90

Jonas PR. 1996. Turbulence and cloud microphysics. *Atmos. Res.* 40:283–306

Kerstein AR. 1991. Linear-eddy modelling of turbulent transport. Part 6. Microstructure of diffusive scalar mixing fields. *J. Fluid Mech.* 231:361–94

Khain AP, Pinsky MB. 1995. Drop inertia and its contribution to turbulent coalescence in convective clouds: part I. Drop fall in the flow with random horizontal velocity. *J. Atmos. Sci.* 52:196–206

Khain AP, Pinsky MB. 1997. Turbulence effects on the collision kernel. II: increase of the swept volume of colliding drops. *Q. J. R. Meteorol. Soc.* 123:1543–60

Khvorostyanov VI, Curry JA. 1999a. Toward the theory of stochastic condensation in clouds. Part I: a general kinetic equation. *J. Atmos. Sci.* 56:3985–96

Khvorostyanov VI, Curry JA. 1999b. Toward the theory of stochastic condensation in clouds. Part II: analytical solutions of the gamma-distribution type. *J. Atmos. Sci.* 56:3997–4013

Knight CA, Miller LJ. 1998. Early radar echoes from small, warm cumulus: Bragg and hydrometeor scattering. *J. Atmos. Sci.* 55:2974–92

Korolev AV, Isaac GA. 2000. Drop growth due to high supersaturation caused by isobaric mixing. *J. Atmos. Sci.* 57:1675–85

Korolev AV, Mazin IP. 1993. Zones of increased and decreased droplet concentration in stratiform clouds. *J. Appl. Meteor.* 32:760–73

Kostinski AB. 2001. On the extinction of radiation by a homogeneous but spatially correlated random medium. *J. Opt. Soc. Am.* 18:1929–33

Kostinski AB, Jameson AR. 2000. On the spatial distribution of cloud particles. *J. Atmos. Sci.* 57:901–15

Annu. Rev. Fluid Mech. 2003.35:183-227. Downloaded from www.annualreviews.org
by Fordham University on 01/19/13. For personal use only.

Kostinski AB, Shaw RA. 2001. Scale-dependent droplet clustering in turbulent clouds. *J. Fluid Mech.* 434:389–98

Kozikowska A, Haman K, Supronowicz J. 1984. Preliminary results of an investigation of the spatial distribution of fog droplets by a holographic method. *Q. J. R. Meteorol. Soc.* 110:65–73

Krueger SK, Su CW, McMurtry PA. 1997. Modeling entrainment and finescale mixing in cumulus clouds. *J. Atmos. Sci.* 54:2697–712

Kulmala M, Rannik U, Zapadinsky EL, Clement CF. 1997. The effect of saturation fluctuations on droplet growth. *J. Aerosol Sci.* 28:1395–409

Lamb D. 2001. Rain production in convective storms. In *Severe Convective Storms*, Meteorol. Monogr. 28, no. 50, ed. CA Doswell III, pp. 299–321. Boston, MA: Am. Meteorol. Soc.

Landau LD, Lifshitz EM. 1980. *Statistical Physics.* Oxford: Butterworth Heinemann

La Porta A, Voth GA, Crawford AM, Alexander J, Bodenschatz E. 2001. Fluid particle accelerations in fully developed turbulence. *Nature* 409:1017–19

Lasher-Trapp SG, Cooper WA. 2000. Comparison of theory and observations of broadening of cloud droplet size distributions in warm cumuli. *Int. Conf. Clouds Precip., 13th*, pp. 90–93. Reno, NV: ICCP

Lawson RP, Cormack RH. 1995. Theoretical design and preliminary tests of two new particle spectrometers for cloud microphysics research. *Atmos. Res.* 35:315–48

Libby PA, Williams FA. 1980. *Turbulent Reacting Flows.* Berlin: Springler-Verlag

Liu Y, Hallett J. 1998. On size distributions of cloud droplets growing by condensation: a new conceptual model. *J. Atmos. Sci.* 55:527–36. Corrigendum. 1998. *J. Atmos. Sci.* 55:1731

Liu Y, You L, Yang W, Liu F. 1995. On the size distribution of cloud droplets. *Atmos. Res.* 35:201–16

Malinowski SP, Zawadzki I, Banat P. 1998. Laboratory observations of cloud–clear air mixing at small scales. *J. Atmos. Ocean. Technol.* 15:1060–65

Manton MJ. 1974. On the motion of a small particle in the atmosphere. *Bound.-Layer Meteorol.* 6:487–504

Manton MJ. 1977. The equation of motion for a small aerosol in a continuum. *Pageoph* 115:547–59

Marshak A, Davis A, Wiscombe W, Cahalan R. 1998. Radiative effects of sub-mean free path liquid water variability observed in stratiform clouds. *J. Geophys. Res.* 103:19557–67

Maxey MR. 1987. The gravitational settling of aerosol particles in homogeneous turbulence and random flow fields. *J. Fluid Mech.* 174:441–65

Maxey MR, Corrsin S. 1986. Gravitational settling of aerosol particles in randomly oriented cellular flow fields. *J. Atmos. Sci.* 43:1112–34

Maxey MR, Riley JJ. 1983. Equation of motion for a small rigid sphere in a nonuniform flow. *Phys. Fluids* 26:883–89

Mazin I. 1999. The effect of condensation and evaporation on turbulence in clouds. *Atmos. Res.* 51:171–74

Monin AS, Yaglom AM. 1975. *Statistical Fluid Mechanics*, Vol. 2. Cambridge, MA: MIT Press

Muschinski A, Lenschow DH. 2001. Future directions for research on meter- and submeter-scale atmospheric turbulence. *Bull. Am. Meteorol. Soc.* 82:2831–43

Oreskes N, Shrader-Frechette K, Belitz K. 1994. Verification, validation, and confirmation of numerical models in the earth sciences. *Science* 263:641–46

Paluch IR, Baumgardner DG. 1989. Entrainment and fine-scale mixing in a continental convective cloud. *J. Atmos. Sci.* 46:261–78

Pinsky MB, Khain AP. 1996. Simulations of drop fall in a homogeneous isotropic turbulent flow. *Atmos. Res.* 40:223–59

Pinsky M, Khain A. 1997a. Formation of inhomogeneity in drop concentration induced by the inertia of drops falling in a turbulent

flow, and the influence of the inhomogeneity on the drop-spectrum broadening. *Q. J. R. Meteorol. Soc.* 123:165–86

Pinsky MB, Khain AP. 1997b. Turbulence effects on droplet growth and size distributions in clouds—a review. *J. Aerosol Sci.* 28:1177–214

Pinsky MB, Khain AP. 1997c. Turbulence effects on the collision kernel. I: formation of velocity deviations of drops falling within a turbulent three-dimensional flow. *Q. J. R. Meteorol. Soc.* 123:1517–42

Pinsky M, Khain AP. 2001. Fine structure of cloud droplet concentration as seen from the Fast-FSSP measurements. Part 1: method of analysis and preliminary results. *J. Appl. Meteorol.* 40:1515–37

Pinsky MB, Khain AP, Levin Z. 1999a. The role of inertia of cloud droplets in the evolution of the spectra during drop growth by diffusion. *Q. J. R. Meteorol. Soc.* 125:553–81

Pinsky M, Khain A, Shapiro M. 1999b. Collision of small drops in a turbulent flow. Part I: collision efficiency. Problem formation and preliminary results. *J. Atmos. Sci.* 56:2585–600

Pinsky M, Khain A, Shapiro M. 2000. Stochastic effects of cloud droplet hydrodynamic interaction in a turbulent flow. *Atmos. Res.* 53:131–69

Pinsky M, Khain A, Shapiro M. 2001. Collision efficiency of drops in a wide range of Reynolds numbers: effects of pressure on spectrum evolution. *J. Atmos. Sci.* 58:742–64

Politovich MK. 1993. A study of the broadening of droplet size distributions in cumuli. *J. Atmos. Sci.* 50:2230–44

Pruppacher HR, Klett JD. 1997. *Microphysics of Clouds and Precipitation.* Dordrecht, The Netherlands: Kluwer

Pu Y, Meng H. 2000. An advanced off-axis holographic particle image velocimetry (HPIV) system. *Exp. Fluids* 29:184–97

Reade WC, Collins LR. 2000. Effect of preferential concentration on turbulent collision rates. *Phys. Fluids* 12:2530–40

Reif F. 1965. *Fundamentals of Statistical and Thermal Physics* Boston, MA: McGraw-Hill

Rogers RR, Brown WOJ. 1997. Radar observations of a major industrial fire. *Bull. Am. Meteorol. Soc.* 78:803–14

Rogers RR, Yau MK. 1989. *A Short Course in Cloud Physics.* Oxford: Pergamon

Saffman PG, Turner JS. 1956. On the collision of drops in turbulent clouds. *J. Fluid Mech.* 1:16–30

Schwartz KW. 1990. Evidence for organized small-scale structure in fully developed turbulence. *Phys. Rev. Lett.* 64:415–18

Seinfeld JH, Pandis SN. 1998. *Atmospheric Chemistry and Physics.* New York: Wiley & Sons

Shaw RA. 2000. Supersaturation intermittency in turbulent clouds. *J. Atmos. Sci.* 57:3452–56

Shaw RA, Kostinski AB, Lanterman DD. 2002. Super-exponential extinction of radiation in a negatively correlated random medium. *J. Quant. Spec. Rad. Trans.* 75:13–20

Shaw RA, Kostinski AB, Larsen ML. 2002b. Towards quantifying droplet clustering in clouds. *Q. J. R. Meteorol. Soc.* 128:1043–57

Shaw RA, Oncley SP. 2001. Acceleration intermittency and enhanced collision kernels in turbulent clouds. *Atmos. Res.* 59/60:77–87

Shaw RA, Reade WC, Collins LR, Verlinde J. 1998. Preferential concentration of cloud droplets by turbulence: effects on the early evolution of cumulus cloud droplet spectra. *J. Atmos. Sci.* 55:1965–76

Shaw RA, Reade WC, Collins LR, Verlinde J. 1999. Reply. *J. Atmos. Sci.* 55:1437–41

She Z-S, Jackson E, Orszag SA. 1990. Intermittent vortex structures in homogeneous isotropic turbulence. *Nature* 344:226–28

Siebert H, Teichmann U. 2000. The behaviour of an ultrasonic under cloud conditions. *Bound.-Layer Meteorol.* 94:165–69

Smith SH, Jonas PR. 1995. Observations of the turbulent fluxes in fields of cumulus clouds. *Q. J. R. Meteorol. Soc.* 121:1185–208

Annu. Rev. Fluid Mech. 2003.35:183-227. Downloaded from www.annualreviews.org
by Fordham University on 01/19/13. For personal use only.

Sreenivasan K, Antonia RA. 1997. The phenomenology of small-scale turbulence. *Annu. Rev. Fluid Mech.* 29:435–72

Srivastava RC. 1989. Growth of cloud drops by condensation: a criticism of currently accepted theory and a new approach. *J. Atmos. Sci.* 46:869–87

Stepanov AS. 1975. Condensational growth of cloud drops in a turbulized atmosphere. *Izv. Atmos. Ocean. Phys.* 11:27–42

Stevens B, Cotton WR, Feingold G. 1998. A critique of one- and two-dimensional models of boundary layer clouds with a binned representation of drop microphysics. *Atmos. Res.* 47/48:529–53

Su C-W, Krueger SK, McMurtry PA, Austin PH. 1998. Linear eddy modeling of droplet spectral evolution during entrainment and mixing in cumulus clouds. *Atmos. Res.* 47/48:41–58

Sundaram S, Collins LR. 1997. Collision statistics in an isotropic particle-laden turbulent suspension. Part 1. Direct numerical simulations. *J. Fluid Mech.* 335:75–109

Tennekes H, Woods JD. 1973. Coalescence in a weakly turbulent cloud. *Q. J. R. Meteorol. Soc.* 99:758–63

Twomey S. 1977. *Atmospheric Aerosols.* Amsterdam, The Netherlands: Elsevier

Uhlig E, Borrmann S, Jaenicke R. 1998. Holographic in-situ measurements of the spatial droplet distribution in stratiform clouds. *Tellus* 50B:377–87

Vaillancourt PA, Yau MK. 2000. Review of particle-turbulence interactions and consequences for cloud physics. *Bull. Am. Meteorol. Soc.* 81:285–98

Vaillancourt PA, Yau MK, Bartello P, Grabowski WW. 2002. Microscopic approach to cloud droplet growth by condensation. Part II: turbulence, clustering and condensational growth. *J. Atmos. Sci.* In press

Vaillancourt PA, Yau MK, Grabowski WW. 2001. Microscopic approach to cloud droplet growth by condensation. Part I: model description and results without turbulence. *J. Atmos. Sci.* 58:1945–64

Vohl O, Mitra SK, Wurzler SC, Pruppacher HR. 1999. A wind-tunnel study of the effects of turbulence on the growth of cloud drops by collision and coalescence. *J. Atmos. Sci.* 56:4088–99

Voth GA, Satyanarayan K, Bodenschatz E. 1998. Lagrangian acceleration measurements at large Reynolds numbers. *Phys. Fluids* 10:2268–80

Wang L-P, Maxey MR. 1993. Settling velocity and concentration distribution of heavy particles in homogeneous isotropic turbulence. *J. Fluid Mech.* 256:27–68

Wang L-P, Wexler AS, Zhou Y. 2000. Statistical mechanical description and modelling of turbulent collision of inertial particles. *J. Fluid Mech.* 415:117–53

Warhaft Z. 2000. Passive scalars in turbulent flows. *Annu. Rev. Fluid Mech.* 32:203–40

Weil JC, Lawson RP, Rodi AR. 1993. Relative dispersion of ice crystals in seeded cumuli. *J. Appl. Meteorol.* 32:1055–73

Woods JD, Drake JC, Goldsmith P. 1972. Coalescence in a turbulent cloud. *Q. J. R. Meteorol. Soc.* 99:758–63

Wyngaard JC. 1988. The effects of probe-induced flow distortion on atmospheric turbulence measurements: extension to scalars. *J. Atmos. Sci.* 45:3400–12

Wyngaard JC. 1992. Atmospheric turbulence. *Annu. Rev. Fluid Mech.* 24:205–33

Zangwill A. 2001. Advances in aggregation. *Nature* 411:651–52

Annu. Rev. Fluid Mech. 2003.35:183-227. Downloaded from www.annualreviews.org
by Fordham University on 01/19/13. For personal use only.

Annual Review of Fluid Mechanics
Volume 35, 2003

CONTENTS

STANLEY CORRSIN: 1920–1986, *John L. Lumley and Stephen H. Davis* 1
AIRCRAFT ICING, *Tuncer Cebeci and Fassi Kafyeke* 11
WATER-WAVE IMPACT ON WALLS, *D. H. Peregrine* 23
MECHANISMS ON TRANSVERSE MOTIONS IN TURBULENT WALL FLOWS, *G. E. Karniadakis and Kwing-So Choi* 45
INSTABILITIES IN FLUIDIZED BEDS, *Sankaran Sundaresan* 63
AERODYNAMICS OF SMALL VEHICLES, *Thomas J. Mueller and James D. DeLaurier* 89
MATERIAL INSTABILITY IN COMPLEX FLUIDS, *J. D. Goddard* 113
MIXING EFFICIENCY IN STRATIFIED SHEAR FLOWS, *W. R. Peltier and C. P. Caulfield* 135
THE FLOW OF HUMAN CROWDS, *Roger L. Hughes* 169
PARTICLE-TURBULENCE INTERACTIONS IN ATMOSPHERIC CLOUDS, *Raymond A. Shaw* 183
LOW-DIMENSIONAL MODELING AND NUMERICAL SIMULATION OF TRANSITION IN SIMPLE SHEAR FLOWS, *Dietmar Rempfer* 229
RAPID GRANULAR FLOWS, *Isaac Goldhirsch* 267
BIFURCATING AND BLOOMING JETS, *W. C. Reynolds, D. E. Parekh, P. J. D. Juvet, and M. J. D. Lee* 295
TEXTBOOK MULTIGRID EFFICIENCY FOR FLUID SIMULATIONS, *James L. Thomas, Boris Diskin, and Achi Brandt* 317
LEVEL SET METHODS FOR FLUID INTERFACES, *J. A. Sethian and Peter Smereka* 341
SMALL-SCALE HYDRODYNAMICS IN LAKES, *Alfred Wüest and Andreas Lorke* 373
STABILITY AND TRANSITION OF THREE-DIMENSIONAL BOUNDARY LAYERS, *William S. Saric, Helen L. Reed, Edward B. White* 413
SHELL MODELS OF ENERGY CASCADE IN TURBULENCE, *Luca Biferale* 441
FLOW AND DISPERSION IN URBAN AREAS, *R. E. Britter and S. R. Hanna* 469

Annu. Rev. Fluid Mech. 2003.35:183-227. Downloaded from www.annualreviews.org
by Fordham University on 01/19/13. For personal use only.

INDEXES
Subject Index 497
Cumulative Index of Contributing Authors, Volumes 1–35 521
Cumulative Index of Chapter Titles, Volumes 1–35 528

ERRATA
An online log of corrections to *Annual Review of Fluid Mechanics* chapters may be found at http://fluid.annualreviews.org/errata.shtml

Annu. Rev. Fluid Mech. 2003.35:183-227. Downloaded from www.annualreviews.org
by Fordham University on 01/19/13. For personal use only.